[156] Chen, S., Lookman, T., Growth kinetics in multicomponent fluids, J. Stat. Phys., 81 (1995), 223–235; Osborn, W. R., Orlandini, E., Swift, M. R., Yeomans, J. M., Banavar, J. R., Lattice Boltzmann study of hydrodynamic spinodal decomposition, Phys. Rev. Lett., 75 (1995), 4031–4034; Wu, Y., Alexander, F. J., Lookman, T., Chen, S., Effects of hydrodynamics on phase transition kinetics in two-dimensional binary fluids, Phys. Rev. Lett., 74 (1995), 3852–3855; Haas, C. K., Torkelson, J. M., Two-dimensional coarsening and phase separation in thin polymer solution films, Phys. Rev. Lett. E, 55 (1997), 3191–3201.

[157] Velasco, E., Toxvaerd, S., Computer simulation of late-stage growth in phase-separating binary mixtures: critical and off-critical quenches, J. Phys.: Condens. Matter, 6 (1994), L205–L209; Velasco, E., Toxvaerd, S., Phase separation in two-dimensional binary fluids: A molecular dynamics study, Phys. Rev. E, 54 (1996), 605–610.

[158] Conveney, P. V., Novik, K. E., Computer simulation of domain growth and phase separation in two-dimensional binary immiscible fluids using dissipative particel dynamics, Phys. Rev. E, 54 (1996), 5134–5141; Kumar, P. B. S., Rao, M., Novel Monte Carlo approach to the dynamics of fluids: single particle diffusion, correlation functions, and phase ordering of binary fluids, Phys. Rev. Lett., 77 (1996), 1067–1070; Emerton, A. N., Coveney, P. V., Boghosian, B. M., Lattice gas simulations of domain growth, saturation, and self-assembly in immiscible fluids and microemulsions, Phys. Rev. E, 55 (1997), 708–720; Weig, P. W. J., Coveney, P. V., Boghosian, B. M., Lattice gas simulations of minority-phase domain growth in binary immiscible and ternary amphiphilic fluids, Phys. Rev. E, 56 (1997), 6877–6888.

Paper received: 1997-10-2
Paper accepted: 1997-10-7

Prof. Dr. K. Binder
Institut für Physik
Johannes-Gutenberg-Universität Mainz
Staudingerweg 7
D-55099 Mainz
Germany

JOURNAL OF
NON-EQUILIBRIUM
THERMODYNAMICS

Offprint

W
DE
G
Walter de Gruyter · Berlin · New York

ıes for the Preparation of Manuscripts

ıd length of contribution

l of Non-Equilibrium Thermodynamics will pu-
:d review articles, papers describing original rese-
ort communications not exceeding 1000 words.

articles will be solicited by the Editors and the
lvisory Board. The articles should provide a cov-
:oretical and of experimental results in one part-
of Non-Equilibrium Thermodynamics.

contributions should contain new and original
search results. The manuscript should not exceed
:en pages (DIN A4).

mmunications are mainly devoted to rapid publi-
:w results. Besides they may be used to discuss
ished in the journal previously.
:ript should not exceed 6 typewritten pages or

for the submission of manuscripts:

the original manuscript and three copies to:
Non-Equilibrium Thermodynamics
ffice
34 21
:rlin

+ 30-260 05-219
-260 05-325
T.editorial@deGruyter.de

ınce procedure for manuscripts

:d papers will be passed on by the Editors to
the Editorial Advisory Board (EAB) for evalua-
embers of the EAB are authorized to review
and accept them for publication. As a rule for a
:cepted it is necessary to obtain the recommen-
o reviewers one of which should be a member
Only papers which have neither been published
r have been submitted for publication to another
e accepted for publication.

e

of the Journal of Non-Equilibrium Thermody-
glish.

manuscripts

:quested only to submit manuscripts which are
ess. This normally will be assured, if the
ommendations are kindly observed.
ıe manuscript should generally follow the rec-
of the "Style Manual" (PUB. R-128.5) of the
itute of Physics.
several key-words should be given which are
nd informative. These key-words will be used
the paper in the subject index of the Journal.
ıuld also include a short abstract of 200 words
:lear indication of the nature and the range of
:ained in the paper.

The **introduction** to the paper should contain a clear definition of the problem being considered.
Wherever possible **theoretical results** should be cited.
The use of the **international system of units** (S.I. units) is required. As far as possible mathematical expressions and symbols should by typed, or inserted neatly in ink.
Only Latin and Greek alphabets are to be used.
Complicated superscripts and subscripts should be avoided by introducing new symbols. Equations should be well aligned and should not be crowded. Avoid repetition of a complicated expression by representing it with a symbol.
Manuscripts should be typed double-spaced on one side of good quality paper with a left-hand margin of 4 cm. The original paper and two copies should be submitted to expedite processing.
The author's name should be written below the title of the manuscript. The author's full postal address, position and affiliation should be given on a separate sheet at the end of the manuscript after the References.
Illustrations like photographs, charts and diagrams should accompany the manuscript and are to be restricted to the necessary minimum. They should be referred to as "Figures" and should be numbered consecutively in the order in which they appear in the text. The figures should have brief captions to make them as informative as possible.

References in the text should be indicated by using arabic numerals in square brackets.

Example: [1]
They should be in numerical order through the text.

The references should be quoted in numerical order at the end of the text. They should include: the names and initials of all authors, the title of the article, the abbreviated title of the journal as listed in the "World List of Scientific Periodicals" (Butterworth, London), the volume number, the year of publication and the page number.

Example:
[7] Mayer, A. B., Smith, R. H., On the Entropy Production Inequality, Physica, 46 (1970), 154.

References to books should include: the name and initials of all authors, the title, edition, volume number and chapter or page, the publisher's name and the place and date of publication.

Example:
[8] Carslaw, H. S., Jaeger, J. C., Operational Methods in Applied Mathematics, 2nd edition, p. 63, Oxford University Press, Oxford, 1963.

Proofs will be sent to the author for correction. At this stage, only typographical errors should be corrected. Substantial changes in the text will be charged to the authors.

20 **offprints** of each paper will be forwarded to the author free of charge. An order form for additional offprints will accompany the proofs.

Manuscripts that are not concisely written or do not conform to the conventions of the journal will be returned to the author.

J. Non-Equilib. Thermodyn.
1998 · Vol. 23 · pp. 1–44

Review Article

Spinodal Decomposition in Confined Geometry

K. Binder
Institut für Physik, Johannes-Gutenberg–Universität Mainz, Mainz, Germany

Registration Number 772

Abstract

When binary mixtures (AB) are quenched from the one–phase region into the unstable part of their miscibility gap, phase separation starts by spontaneous amplification of concentration fluctuations ("spinodal decomposition"). This growth of A–rich and B–rich domains and their morphology is distinctly modified when one considers mixtures confined in thin film geometry between planar parallel walls, or confined in cylindrical geometry in pores. The boundary effects created by this confinement on the mixture can imply formation of a layered structure parallel to the walls ("surface directed spinodal decomposition") and can also involve an intricate interplay with wetting phenomena. In porous media the randomness of the pore structure presents an additional complication.

This review presents a tutorial introduction to these phenomena, comparing them also to spinodal decomposition and coarsening in the bulk. Emphasis is on theoretical concepts and on numerical simulations, but pertinent experiments are also briefly mentioned, and a discussion of open problems is given.

1. Introduction and Overview

In the industrial processing of materials it is very common that by a change of external control parameters (temperature T, pressure p, etc.) one can bring a binary (AB) mixture (or a multi-component mixture, respectively) from a state in the one-phase region, where the system is homogeneously miscible not only on macroscopic length scales but even down to molecular scales, to a state inside a miscibility gap in the (thermal equilibrium) phase diagram of the system. Then thermal equilibrium requires the coexistence of (macroscopic) domains of the various phases, and it is of great interest to consider the kinetic pathways how the considered system develops from its initial, now unstable, state, which is homogeneous apart from statistical fluctuations, to this macroscopically inhomogeneous concentration distribution.

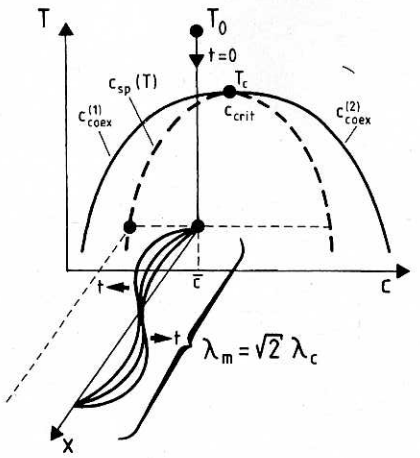

Fig. 1: Schematic description of a quenching experiment that leads to spinodal decomposition of a binary mixture: one starts at a temperature T_0 such that the system is in thermal equilibrium for times $t < 0$ at the chosen average concentration $\bar{c}$ of one species (say, A). At time $t = 0$, the system is suddenly cooled to a temperature T underneath the coexistence curve (consisting of two branches $c^{(1)}_{coex}$, $c^{(2)}_{coex}$ that merge at a critical point T_c, c_{crit}). If the state point $(\bar{c}, T)$ lies inside of the spinodal curve $c_{sp}(T)$, then the linear theory [1, 2] predicts that in the bulk of the system long wavelength concentration fluctuations (exceeding a critical wavelength λ_c) are unstable, and grow spontaneously in time (maximum growth rate occurs initially for $\lambda_m = \sqrt{2}\lambda_c$). This is schematically indicated in the figure, where a growth of a single concentration wave in the x-direction is shown.

Figure 1 depicts one of the basic ideas [1–7] that has emerged for such processes. Introducing an effective (coarse-grained) free energy of locally homogeneous states $F'(c)$ inside the miscibility gap, one can distinguish between metastable states {for which $\partial^2 F'(c)/\partial c^2 > 0$} and unstable states {for which $\partial^2 F'(c)/\partial c^2 < 0$}, separated by the "spinodal curve", $c_{sp}(T)$, for which $\partial^2 F'(c)/\partial c^2|_{c = c_{sp}(T)} = 0$. It is thought that the decay of metastable states is started by the spontaneous nucleation of "heterophase fluctuations", i.e. droplets of the minority phase are growing in the background of the majority phase [3–11]. In the unstable regime, in contrast, it is thought that random long wavelength concentration fluctuations get amplified as the time after the quench passes. In the simplest linearized version of the theory [1,2], all concentration waves whose wavelength λ exceeds a critical wavelength λ_c grow exponentially with time, independent of each other. Now it is well-known [3, 5, 8, 12, 13, 14, 15] that the sharp spinodal curve in the phase diagram in Figure 1 is a somewhat ill-defined concept (e.g. because in the two-phase region the coarse-grained free energy $F'(c)$ depends somewhat [13] on the length scale over which the coarse-graining is performed). This is true for most systems (notable exceptions are systems with forces of sufficiently long range so nucleation gets suppressed and mean-field theory gets strictly valid [12] or equivalent

problems such as polymer mixtures in the limit where the molecular weights tend to infinity [15]). Thus, the critical singularities associated with $c_{sp}(T)$, namely both $\lambda_c \to \infty$ as $c \to c_{sp}(T)$ from the unstable side [1, 2] while the critical droplet radius $R \to \infty$ as $c \to c_{sp}(T)$ from the metastable side [16, 17], are rounded off: $c_{sp}(T)$ is smeared out from a sharp line into a fuzzy region where a gradual transition from nucleation and growth (on the metastable side) to (nonlinear) spinodal decomposition and coarsening (on the unstable side) occurs [3, 5, 10, 15]. This nonlinear spinodal decomposition mechanism means that already the initial amplitudes of the concentration waves in Figure 1 are so large that these waves are strongly interacting. As a result, there is no exponential growth of the scattering intensity (which is proportional to the mean square amplitude of the concentration waves) at a fixed wavelength λ_m of maximum growth, but rather the maximum scattering intensity occurs at wavelengths $\lambda_m(t)$ which shift to larger and larger length scales as time passes, $\lambda_m(t \to \infty) \to \infty$. Only for polymer mixtures with large enough molecular weights has it been possible to observe an initial stage of exponential growth at constant λ_m, before the coarsening due to the nonlinear effects sets in [18, 19]. Thus, "spinodal decomposition" in its original meaning [1, 2] (i.e., the behavior of the linearized theory emphasized in Fig. 1) is rarely observed, rather one understands by spinodal decomposition now the continuous growth of the phase separated structure from mesoscopic scales {where the growth starts immediately after the quench, $\lambda_m(0)$} to macroscopic scales. Understanding this behavior in quantitative detail still is a problem [3–7]: while it has been suggested long ago that there is a simple dynamic scaling of the structure factor [20, 21] {q is the wavenumber of the scattering, d the dimensionality of the system}

$$S(q, t) = [\lambda_m(t)]^d \tilde{S}\{q\lambda_m(t)\}, \tag{1}$$

development of a quantative theory for both the scaling function $\tilde{S}$ and the characteristic length scale $\lambda_m(t)$ is difficult, though there are various simple arguments yielding that asymptotically for large times t $\lambda_m(t)$ should be a power law in time. E.g., for vanishing volume fraction of the minority phase the Lifshitz-Slezov [22, 23] evaporation-condensation mechanism predicts

$$\lambda_m(t) \propto t^{1/3}, \text{ independent of } d \text{ [24]}. \tag{2}$$

For fluids, however, the droplet diffusion-coagulation mechanism (also called "Brownian coalescence") predicts [20]

$$\lambda_m(t) \propto t^{1/d}, \tag{3}$$

and mechanisms invoking hydrodynamic flow of interconnected structures imply [25, 26], in the so-called "viscous hydrodynamic" regime [7]

$$\lambda_m(t) \propto t,\ d = 3 \text{ (Ref. 25)},\ \lambda_m(t) \propto t^{1/2},\ d = 2 \text{[Ref. 26]}. \tag{4}$$

Finally, in the so-called "inertial hydrodynamic" regime [7, 27] {where $\lambda(t) \ll \eta^2/\rho\sigma$ where η is the viscosity, ρ the density and σ the interfacial tension} one predicts

$$\lambda_m(t) \propto t^{2/3}, \text{ independent of } d. \tag{5}$$

While equation (2) can also be obtained from the (purely diffusive) nonlinear Cahn-Hilliard equation [28], the extension of the Lifshitz-Slezov theory to nonzero volume fraction ϕ of the minority phase {in order to understand how the prefactor in equation (2) depends on ϕ} despite many attempts is an unsolved problem [7], and one cannot describe accurately the nonasymptotic approach to these presumably universal power laws yet, nor possible crossovers between them, and the accurate prediction of scaling functions $\tilde{S}$ is even more difficult [7, 29] and possibly has to rely on numerical techniques [30, 31]. It should be noted that these numerical techniques (in particular the molecular dynamics method where one simply integrates Newton's laws for all the particles in the model system [32]) may suffer from accuracy problems [33], and thus a number of recent estimates of growth exponents in the literature are probably not meaningful [33]. Also the experimental study of equations (1)–(4) is still a matter of current debate [34–39]. Solid mixtures—for which the concept of spinodal decomposition originally [1, 2] was introduced!—pose particular problems, since elastic interactions may lead to pinning effects in the growth [36], shape transitions of the growing precipitations (e.g. from spherical to cubic shape [37]) or to precipitate "rafting" [38] (i.e., directional coarsening). Fluid mixtures also are delicate if the two fluids have very different viscosities, e.g. in polymer solutions [39] or polymer blends where one constituent is close to a glass transition [40], the slow component may form a sponge-like network which supports stress and thus eliminates the velocity field and the hydrodynamic growth mechanism based on it, leading again to a $t^{1/3}$ growth law. It also is of great interest to correlate the time evolution of the structure factor with the evolution of the interconnected interfaces in the system, which can be visualized by laser scanning confocal microscopy [41]. Finally we emphasize that one is not only interested in the phase separation kinetics for a fluid at rest but also for fluids exposed to (shear) flow [42, 43]. All these problems are beyond the scope of the present article.

The fact that due to these problems (role of hydrodynamic or elastic long range interactions, effects of strong dynamic asymmetry between the constituents of a mixture, slow transient approach to asymptotic power laws, etc.) spinodal decomposition in the bulk is still incompletely understood must be kept in mind when one considers phase separation in confined geometry. The first effect that needs consideration is that the phase diagram of a confined system, e.g. a thin film, differs from the bulk [44–50]. This change of the thermodynamic equilibrium conditions, which one needs to understand because they act as driving forces for the phase separation kinetics, results from an interplay of surface effects [50–57] and finite size effects [45, 51, 58, 59, 60, 61]. Depending on the surface effects due to the two boundaries of a film, rather different equilibrium conditions may result, as sketched in Figure 2. We here do allow for the general situation that the two surfaces confining the film differ in their nature, e.g. the upper surface is simply a free surface against air, or a solid wall which may differ in chemical nature from the substrate providing the lower surface. Truly long-range concentration correlations can then develop only in the directions parallel to the walls, and hence sharp phase transitions involve lateral phase separation, with interfaces oriented perpendicular to the walls {cases (a), (b), (e)}. The different cases sketched in Figure 2 distinguish whether the surfaces are wetted by the phases that are energetically

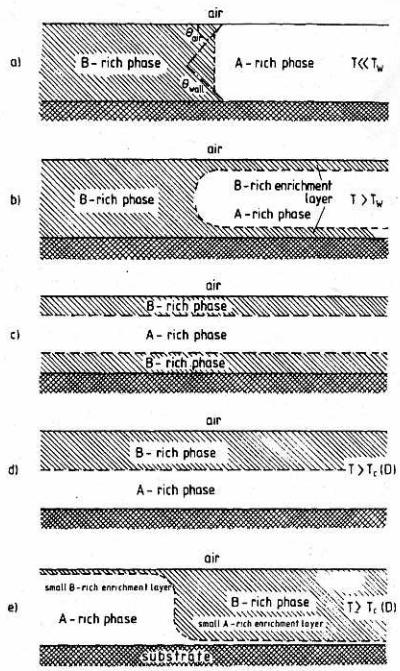

Fig. 2: Schematic description of the equilibrium structure of unmixed binary mixtures (AB) in thin film geometry, assuming that the lower surface is provided by a solid substrate, the upper surface being air or (in general) a different type of solid wall than the substrate. Cases (a)–(c) refer to the case that the B-rich phase is energetically preferred by both surfaces, while cases (d), (e) refer to the case where the B-rich phase is preferred by the upper surface only, while the substrate prefers the A-rich phase. Note that cases (c), (d) describe the one-phase region of the thin film also, simply the interfaces between A-rich and B-rich "phases" are very diffuse and sharpen only gradually (by a smeared-out, rounded transition in the vicinity of the bulk tranistion temperature) when one brings the system inside the coexistence curve of the bulk. Sharp phase transitions in the film then involve lateral phase separation, i.e. a transition from case (c) to case (a) or (b), or from case (d) to case (e). For further explanations see text. From Binder *et al.* [49].

preferred or not. Cases (a)–(c) assume that both walls prefer the B-rich phase. Below the wetting transition [51–57, 62] temperature T_w (which we assume to be the same for both walls, for simplicity) the interface which is perpendicular to the walls in the interior of the film meets the walls under a nonzero contact angle θ_{wall}, while above the wetting temperature T_w the contact angle is zero, and hence the interface bends gradually over, since the A-rich phase is coated with a "wetting layer" {or surface-enrichment layer of the B-rich phase, respectively: note that in thin films with finite thickness D the transition from case (a) to case (b) is not sharp, but also rounded [49, 50], since a sharp wetting transition ideally involves formation of a macroscopically thick wetting layer,

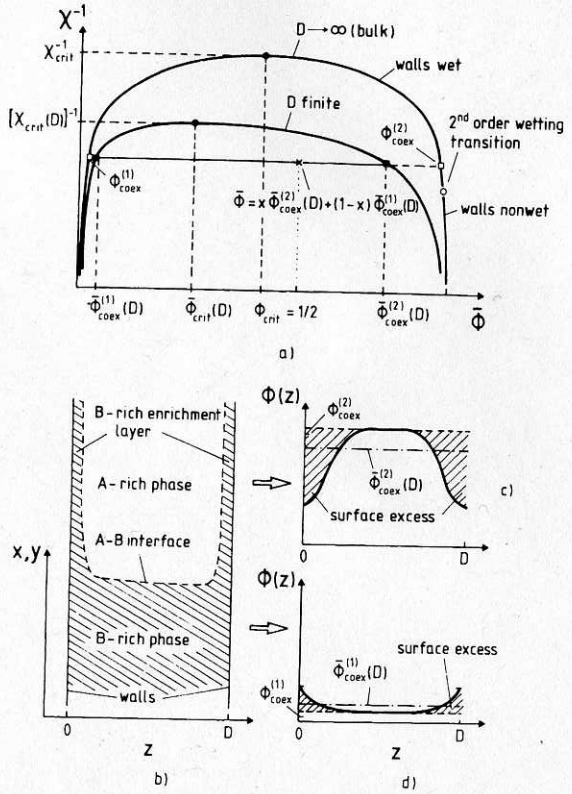

Fig. 3: (a) Qualitative phase diagram of a symmetrical binary (A, B) mixture both in a thin film of the thickness D and in semi-infinite geometry ($D \to \infty$), in the plane of variables inverse effective interaction parameter χ^{-1} (for polymer blends χ is called the Flory-Huggins parameter [50]) and average relative concentration $\bar{\phi}$ of A in the system. Assuming a symmetric mixture in the bulk ($D \to \infty$), the critical concentration $\phi_{crit} = 1/2$, and for $\chi^{-1} < \chi_{crit}^{-1}$ the concentrations $\phi_{coex}^{(1)}$, $\phi_{coex}^{(2)}$ of the two coexisting phases are related by the symmetry relation $\phi_{coex}^{(2)} = 1 - \phi_{coex}^{(1)}$. Assuming a preferential attraction of one species (B) by the walls, this symmetry is broken, andboth the critical concentration $\bar{\phi}_{crit}(D)$ and the concentration atthe A-rich branch of the coexistence curve $\bar{\phi}_{coex}^{(2)}(D)$ are shifted towards smaller concentration, as compared to the bulk. With short range forces at the wall, and unchanged pairwise interactions between atoms of the mixture near the wall, one expects a second-order wetting transition at a temperature $T_w < T_{cb}$ in the semi-infinite system, but this transition is rounded in the thin film geometry. (b) Schematic description of a state of the thin film for a concentration $\bar{\phi}$ inside of the coexistence curve, $\phi_{coex}^{(1)}(D) < \bar{\phi} < \bar{\phi}_{coex}^{(2)}(D)$ (e.g. the point marked by a cross in the phase diagram, part (a)). Then the film is inhomogeneous in the x, y-directions parallel to the walls, the A-rich part of the film in equilibrium being separated from the B-rich part by a single A-B interface running perpendicular to the film. The relative amounts of A-rich (x) and B-rich ($1-x$) phases are simply given by the lever rule, $\bar{\phi} = x\phi_{coex}^{(2)}(D) + (1-x)\phi_{coex}^{(1)}(D)$, with $0 < x < 1$. Here we assume that the film thickness D is much larger than the interfacial thickness w and so the A-rich phase has enrichment layers of the B-rich phase "coating" the walls of the thin film. (c) Concentration profile $\phi(z)$ in the (z)-direction across the film in the A-rich phase. Here the shaded area denotes the surface excess ϕ_s. (d) Same as (c) but for the B-rich phase. From Flebbe *et al.* [48].

which does not fit into the thin film, of course}. Cases (d), (e) refer to the case where the upper surface prefers the B-rich phase while the lower surface prefers the A-rich phase, and thus an A-B-interface parallel to the walls is stabilized in the thin film. The phase transition at $T_c(D)$ then can be viewed as an interface binding-unbinding transition, for $T > T_c(D)$ the interface is unbound from the walls, freely fluctuating in the center of the film [46, 47] (case (d)), while for $T < T_c(D)$ it is bound to the walls {case (e)}. Note that in the limit of very thick films ($D \to \infty$) this transition temperature $T_c(D)$ does not converge to the critical temperature T_{cb} of bulk phase separation but rather to the wetting transition temperature T_w [46, 47]. In contrast, the transition for symmetric walls from state (c) above $T_c(D)$ to state (b) below $T_c(D)$ does converge to the bulk transition temperature for thick films, $T_c(D \to \infty) \to T_{cb}$.

Of course, the sharp $A-B$ interfaces in Figure 2 should not be taken literally —actually one expects smooth concentration profiles across the film, Figure 3, and the concentration near the walls always is inhomogeneous. If the energetic preference for the B-components at the walls is not very strong, the incompatibility is reduced at the walls in both phases, due to the "missing neighbour" effect. Even if the mixture would be perfectly symmetric in the bulk, the energetic preference of the walls for one component breaks this symmetry, and hence there is no mirror symmetry between the profiles of the coexisting A-rich and B-rich phases in the thin film. Consequently, there is also a shift of the critical concentration $\bar{\phi}_{crit}(D)$ relative to the critical concentration ϕ_{crit} in the bulk, in addition to the shift of the critical temperature $T_c(D)$. Typically, confinement enhances the compatibility of the components, and so $T_c(D) < T_{cb}$ (for a mixture with an upper consolute point).

Surface enrichment of the preferred component at the walls then also has a pronounced effect on the dynamics of phase separation in thin films [50, 63–101]. Figure 4 shows typical experimental observations [74], and Figure 5 shows related results of numerical simulations [83]. While in the bulk the wavevectors of the fluctuation that are

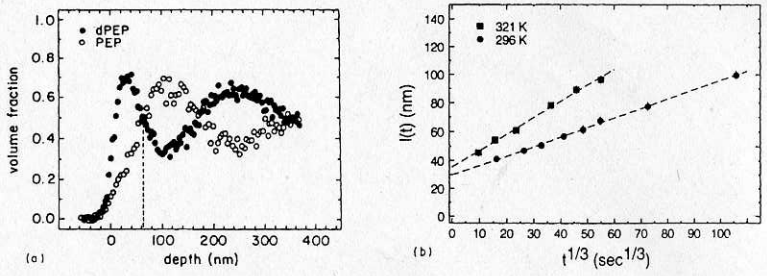

Fig. 4: (a) Volume fraction of deuterated poly (ethylenepropylene), dPEP (full dots) and protonated PEP (open circles) versus depth, for a degree of polymerization $N \approx 2300$ for both constituents, after a 4 h quench to $T = 294$K ($T_{cb} = 365$K). Profiles are obtained with the time of flight forward recoil spectroscopy (TOF-FRES). The dashed line indicates the surface domain thickness $l(t)$. (b) Plot showing the growth of the surface domain thickness $l(t)$ as $t^{1/3}$. From Krausch *et al.* [74]

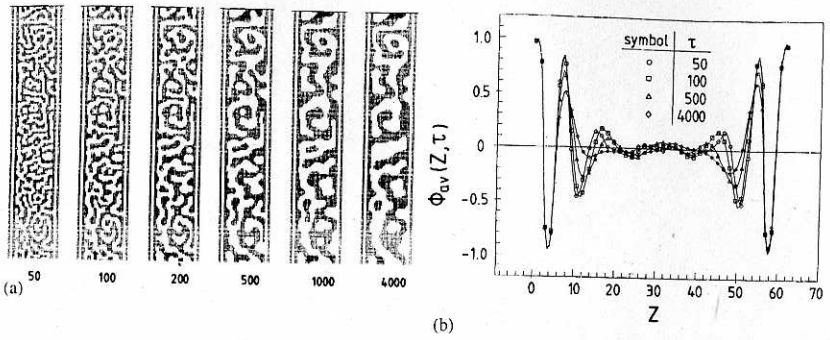

Fig. 5: (a) Snapshot pictures of the time evolution from one discrete Euler implementation (with $\Delta X = 1.5, \Delta\tau = 0.05$) of the partial differential equation describing nonlinear spinodal decomposition (i.e., Eq. (19) below). A square lattice in a $D \times L$ geometry is chosen, with $L = 600$ and $D = 60$. The snapshots refer to scaled times (from left to right) $\tau = 50$, 100, 200, 500, 1000 and 4000. Positive values of the order parameter $\phi(\vec{X}, \tau) = 2c(\vec{X}, \tau) - 1$, where $c(\vec{X}, \tau)$ is the local concentration at time τ, are shown in black while negative values are not marked. The parameters describing the boundary condition at the surface (Eq. (42) below) are chosen as $\gamma = 4$, $g = -4$, and $h_1 = 4$, corresponding to an incompletely wet static equilibrium in a semi-infinite geometry. (b) Averaged order parameter profiles $\phi_{av}(Z, \tau)$ plotted vs. the dimensionless distance Z from the first wall for four different scaled times as indicated, for the same choice of parameters as in (a). Data are obtained as an average over 2000 independent initial conditions. From Puri and Binder [83].

amplified during the initial stages of phase separation after the quench are randomly oriented, giving rise to the characteristic interconnected seaweed-like structure of the growing domains, near the walls wavevectors are oriented perpendicular to the walls and amplitudes are chosen such that the boundary conditions at the walls are fulfilled [63]. Since the characteristic layered structure of these surface-directed concentration waves have been detected in first experiments [66], a lot of activity has been devoted towards a closer investigation of these phenomena [50, 63–101]. Most of experimental studies were performed for polymeric systems, since the large characteristic lengths of the latter are convenient for several techniques of investigation; but related phenomena are expected for small molecular mixtures, too. In this context we draw attention to the point that many elements that do not form miscible solid alloys in the bulk can form mixed two-dimensional alloys confined to a surface layer [102], while in miscible metallic alloys it often happens that one component segregates to the surface [103].

As a last topic of this section, we discuss phase separation in porous media [104–120]. The first approaches [104–107] stressed the randomness of the pore structure (typically one may bring the binary mixture in a porous material like Vycor glass or various aerogels [106, 108, 109, 110]) and qualitatively a description of the phase transition in terms of the random field Ising model [121, 122] was attempted. Thus,

the two components (A, B) of the binary mixture are represented by the two orientations of an Ising spin [3, 5], and the random surface of the porous material (which again will energetically prefer one component) is described by a randomly quenched, uncorrelated random field acting on the Ising spins. Obviously, such a description can make sense only if one considers length scales of concentration correlations which are much larger than the typical diameters of the pores in the network, and thus one might expect that this description will be useful only in the immediate neighborhood of the critical point (which is shifted both in temperature and composition relative to the bulk phase diagram without the porous material [108]). The opposite view concentrates on the wetting behavior on the walls inside of a single straight cylindrical pore [113–119]. Ultimately it is clear that a full understanding must combine the behavior of such straight single pores with a realistic description of the random structure of the pore network in the porous material [119, 120], but one is still far from a full solution to that problem. A particularly interesting situation occurs also for the phase separation of $He^3 - He^4$ mixtures inside pores [110, 111, 112], remembering that in bulk $He^3 - He^4$ mixtures one phase is a normal fluid and the other phase is a superfluid. It has been predicted [111] that in the porous material the phase diagram gets substantially modified, the tricritical point disappears and phase separation occurs entirely within the superfluid phase. This system will remain outside of our further considerations, however.

When one considers a single cylindrical pore (or the related problem of a single two-dimensional strip of width D bounded by two one-dimensional "walls" [123]) one must take into account the specific effects of quasi-one-dimensional systems as soon as the domain linear dimension $l(t)$ has grown to the diameter D of the pore (or strip, respectively), see Figure 6. One-dimensional systems do not have phase transitions with short range forces, and therefore phase separation ultimately must stop when the domain size reaches the finite equilibrium value of the correlation length $\xi_\parallel$ to the walls of the pore (or strip, respectively) [124]. This length is controlled by the interfacial tension f_{int} between the A-rich and B-rich domains, i.e.

$$\xi_\parallel \propto D^{1/2} \exp(f_{\text{int}} D / k_B T), \; d = 2, \tag{6}$$

$$\xi_\parallel \propto \exp(f_{\text{int}} \pi D^2 / 4 k_B T), \; d = 3. \tag{7}$$

Since in the intermediate stage of growth in Figure 6 the flat domain walls can be rather metastable (this state is called "plug phase" or "capsules" if the walls are wetted [113]), one needs two walls to meet by diffusion in order to annihilate the domain enclosed by them, this stage of domain growth is expected to be very slow, if the system behaves purely diffusive. However, in fluid mixtures in this quasi-one dimensional geometry hydrodynamic mechanisms again seem to be very important [116].

After this broad survey over the phenomena discussed in this article, we now treat a few aspects in more detail: in Section 2 we recall the basic aspects of spinodal decomposition in the bulk, while in Section 3 we discuss the theoretical modelling of the surface effects. In Section 4 we summarize the main findings obtained for surface-directed

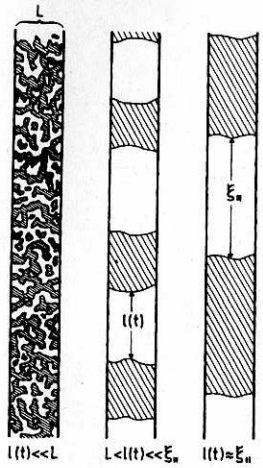

Fig. 6: Schematic description of domain growth of a binary (A, B) mixture in a cylindrical pore of diameter L, assuming essentially "neutral" walls of the pore (no energetic preference for one component), and a volume fraction ϕ_A of A near 50%. The system decomposes for $T \ll T_{cb}$ in two types of domains, B-rich (shaded) and A-rich (white). Domain walls are indicated by thin solid lines. Three stages of domain growth are indicated: in the first stage (left part), the typical linear dimension of domains $l(t)$ is much smaller than L. The process of domain growth is similar to standard (nonlinear) spinodal decomposition in this stage. In the second stage, $l(t)$ is larger than L but smaller than the correlation length $\xi_\parallel$ in the thermal equilibrium (middle part). In the last stage (right part), the domain size $l(t)$ in the direction parallel to the walls of the pore saturates at its equilibrium value $\xi_\parallel$. From Albano *et al.* [123]

spinodal decomposition from the numerical modelling so far. Section 5 gives some more details on the work devoted to spinodal decomposition in straight pores, while Section 6 gives some final discussion including comparison with experiment.

2. The Cahn-Hilliard-Cook Nonlinear Diffusion Equation

We first consider a macroscopic volume V, disregarding any surface effects and introduce a (coarse-grained) concentration field $c(\vec{x})$, which is obtained by averaging the local concentration (which is unity or zero on the atomistic scale, depending on whether we encounter an A-atom or B-atom) over a length scale large in comparison to atomic diameters but small in comparison to the correlation length ξ_b of concentration fluctuations in bulk equilibrium. The point $\vec{x}$ is the center of gravity of the volume region over which this averaging is performed. One expects that then the microscopic (i.e. atomistic) Hamiltonian of the mixture can be replaced by an effective free energy functional

$$\frac{\Delta F\{c(\vec{x})\}}{k_B T} = \int_V d^d x \{f_{cg}[c(\vec{x})]/k_B T + \frac{1}{2d} r^2 [\nabla c(\vec{x})]^2\}, \tag{8}$$

where $f_{cg}(c)$ is the coarse-grained free energy density, normalized with the temperature, and the term $\frac{1}{2d} r^2 [\nabla c(\vec{x})]^2$ accounts for the free energy cost of inhomogeneous concentration distributions. Being interested in slowly varying concentration fields, higher order gradient terms are omitted from the start. Considering atomistic models for mixtures explicitly, one can interpret r as the range of the effective interactions that drive the unmixing [3, 125]. Since equation (8) makes only sense if ξ_b is much larger than interatomic distances, we have to consider the vicinity of the bulk critical temperature T_{cb}, where $c(\vec{x})$ does deviate only a little from the critical concentration c_{crit}, and then one can assume the Landau expansion for $f_{cg}(c)$,

$$f_{cg}(c) = f_0 + \frac{1}{2} A (c - c_{crit})^2 / c_{crit}^2 + \frac{1}{4} B (c - c_{crit})^4 / c_{crit}^4 \tag{9}$$

where f_0, $B > 0$ are constants, while $A \propto (T/T_{cb} - 1) < 0$ for $T \propto T_{cb}$ and changes sign at T_{cb}.

We now turn to the dynamics of the concentration field $c(\vec{x}, t)$, assuming the simplest case (appropriate for solid mixtures only) where the only processes to consider are purely diffusive (in fluids the velocity field $\vec{u}(x, t)$ needs to be included as a second variable [126, 127]!). Since in the total volume V the average concentration

$$\bar{c} = (1/V) \int_V d\vec{x} c(\vec{x}, t) \tag{10}$$

is conserved, the time-dependent concentration field $c(\vec{x}, t)$ satisfies a continuity equation,

$$\partial c(\vec{x}, t)/\partial t + \nabla \cdot \vec{j}(\vec{x}, t) = 0, \tag{11}$$

where $\vec{j}(\vec{x}, t)$ is the concentration current density. In the spirit of standard nonequilibrium thermodynamics [128], $\vec{j}(\vec{x}, t)$ is assumed to be proportional to the gradient of the local chemical potential difference $\mu(\vec{x}, t)$,

$$\vec{j}(\vec{x}, t) = -M \nabla \mu(\vec{x}, t), \tag{12}$$

M being a mobility.

In thermal equilibrium the chemical potential difference is given as a partial derivative of the free energy of mixing, $F(c, T)$,

$$\mu = (\partial F/\partial c)_T. \tag{13}$$

Remember that the condition for two-phase coexistence is the equality of chemical potential differences in both phases,

$$\mu_1 = (\partial F/\partial c)_T|_{c_{coex}^{(1)}} = \mu_2 = (\partial F/\partial c)_T|_{c_{coex}^{(2)}} \tag{14}$$

We generalize equation (13) to an inhomogeneous nonstationary situation far from equilibrium, where both $c(\vec{x}, t)$ and $\mu(\vec{x}, t)$ depend on space and time, by defining $\mu(\vec{x}, t)$ as a functional derivative of the free energy functional ΔF in equation (8)

$$\mu(\vec{x}, t) \equiv \delta[\Delta F\{c(\vec{x}, t)\}]/\delta c(\vec{x}, t). \tag{15}$$

Using equation (8) in equation (15) yields

$$\mu(\vec{x}, t) = (\partial f_{cg}(c)/\partial c)_T - \frac{1}{d} r^2 k_B T \nabla^2 c(\vec{x}, t), \tag{16}$$

and using this result in equations (11), (12) one obtains the Cahn-Hilliard [1, 2] nonlinear diffusion equation,

$$\frac{\partial c(\vec{x}, t)}{\partial t} = M \nabla^2 \left\{ \left(\frac{\partial f_{cg}[c(\vec{x}, t)]}{\partial c} \right)_T - \frac{1}{d} r^2 k_B T \nabla^2 c(\vec{x}, t) \right\}. \tag{17}$$

Using equation (9) and defining $(c(\vec{x}, t) - c_{crit})/c_{crit} = \psi(\vec{x}, t)$ as order parameter of the transition, one obtains the conserved version of the time dependent Ginzburg-Landau equation

$$\frac{\partial \psi(\vec{x}, t)}{\partial t} = k_B T M \nabla^2 \left\{ A\psi(\vec{x}, t) + B\psi^3(\vec{x}, t) - \frac{1}{d} r^2 \nabla^2 \psi(\vec{x}, t) \right\}. \tag{18}$$

By suitable rescaling of the scales of time, space and the order parameter one can absorb all constants $M, A, B, r^2 k_B T$ in the scales of the scaled time τ, scaled position $\vec{X}$, and scaled order parameter ϕ(∇ now means derivates with respect to $\vec{X}$)

$$\frac{\partial \phi(\vec{X}, \tau)}{\partial \tau} = \nabla^2 \left\{ -\phi(\vec{X}, \tau) + \phi^3(\vec{X}, \tau) - \frac{1}{2} \nabla^2 \phi(\vec{X}, \tau) \right\}. \tag{19}$$

This rescaling is achieved by measuring lengths in terms of twice the correlation length ξ_b^{coex} of bulk concentration fluctuations at the coexistence curve, remembering $A < 0$ for $T < T_{cb}$,

$$\xi_b^{coex} = r/\sqrt{(-2dA)}, \quad \vec{X} \equiv \vec{x}/(2\xi_b^{coex}), \tag{20}$$

the order parameter is measured in terms of its value ψ_b at the coexistence curve,

$$\psi_b = \sqrt{-A/B}, \quad \phi(\vec{X}, \tau) \equiv \psi(\vec{x}, t)/\psi_b, \tag{21}$$

and the time is rescaled by a characteristic relaxation time t_{rel},

$$t_{rel} = (-A)/[4k_B T M (\xi_b^{coex})^2], \quad \tau \equiv t/t_{rel}. \tag{22}$$

One immediately obvious drawback of the nonlinear Cahn-Hilliard equation is its completely deterministic character, which implies that random statistical fluctuations are disregarded (except from fluctuations included in the initial condition, the state at temperature T_0 where the quench starts). This problem can be remedied [129] by adding a random force term $\eta_T(\vec{x}, t)$ to equation (17),

$$\frac{\partial c(\vec{x}, t)}{\partial t} = M \nabla^2 \left\{ \left(\frac{\partial f_{cg}[c(\vec{x}, t)]}{\partial c} \right)_T - \frac{1}{d} r^2 k_B T \nabla^2 c(\vec{x}, t) \right\} + \eta_T(\vec{x}, t). \tag{23}$$

Here $\eta_T(\vec{x}, t)$ is assumed to be a delta-correlated Gaussian noise, and its mean square amplitude $\langle \eta_T^2 \rangle_T$ is then linked to the mobility M via a fluctuation-dissipation relation [126]

$$\langle \eta_T(\vec{x}, t) \eta_T(\vec{x}', t') \rangle_T = \langle \eta_T^2 \rangle_T \nabla^2 \delta(\vec{x} - \vec{x}') \delta(t - t'), \tag{24}$$

$$\langle \eta_T^2 \rangle_T = 2k_B T M. \tag{25}$$

Equations (23)–(25) are the basic starting point for the theoretical description of spinodal decomposition, including both statistical fluctuations and nonlinear effects. However, coupling to other dynamic variables (solid alloys: atomic displacement field; fluids: velocity field; polymers: conformational degrees of freedom; etc.) is disregarded throughout. Note also that in taking the step from equations (11), (12) to equation (17) we have neglected any possible concentration dependence of the mobility M, which is also not true in general but should be reasonable near T_{cb} where the concentration differences of interest are small since $\psi_b = (c_{coex} - c_{crit})/c_{crit} \ll 1$.

Despite these many simplifying assumptions, equations (23)–(25) withstand any analytic solution. Here we shall neither discuss the large body of numerical work, dealing with equations (23)–(25) [3, 4, 5, 7, 30, 130] nor related models like the Kawasaki [131] spin-exchange kinetic Ising model [132]. Rather we emphasize only the simplest approach, namely the Cahn [1, 2] linearized theory. Despite the fact that this theory is rarely accurate, as emphasized already in the introduction, it provides a useful first orientation. Thus we assume that in the initial stages of unmixing the fluctuation around the average concentration $\bar{c}$

$$\delta c(\vec{x}, t) \equiv c(\vec{x}, t) - \bar{c} \tag{26}$$

is small everywhere in the system. This assumption typically is not true since $c(\vec{x}, t)$ is obtained from averaging over a volume that is small in comparison with ξ_b^d, as mentioned above. If we make this assumption nevertheless, we obtain from equation (17) by expanding $\partial f_{cg}/\partial c$ to first order in ∂c

$$\frac{\partial}{\partial t} \delta c(\vec{x}, t) = M \nabla^2 \left\{ (\partial^2 f_{cg}(c)/\partial c^2)_{T, c=\bar{c}} - \frac{1}{d} r^2 k_B T \nabla^2 \right\} \delta c(\vec{x}, t). \tag{27}$$

For simplicity, here also the random force term has been neglected. Introducing Fourier transforms

$$\partial c_{\vec{q}}(t) = \int d^d \vec{x} \exp(i\vec{q} \cdot \vec{x}) \, \delta c(\vec{x}, t), \tag{28}$$

equation (27) becomes

$$\frac{\partial}{\partial t} \delta c_{\vec{q}}(t) = -Mq^2 \left\{ (\partial^2 f_{cg}(c)/\partial c^2)_{T, c=\bar{c}} + \frac{1}{d} r^2 k_B T q^2 \right\} \delta c_{\vec{q}}(t). \tag{29}$$

Equation (27) is solved by a simple exponential relaxation

$$\delta c_{\vec{q}}(t) = \delta c_{\vec{q}}(0) \exp[R(\vec{q})t] \tag{30}$$

with the rate factor $R(\vec{q})$ given as

$$R(\vec{q}) = -k_B T M q^2 \left[(\partial^2 f_{cg}(c)/\partial c^2)/k_B T + \frac{r^2}{d} q^2 \right]. \tag{31}$$

The equal-time structure factor $S(\vec{q}, t)$ at time t after the quench, a quantity experimentally accessible via the small angle scattering of neutrons, X-rays or light [4, 6], then becomes

$$S(\vec{q}, t) \equiv \langle \delta c_{-\vec{q}}(t) \delta c_{\vec{q}}(t) \rangle_T = S_{T_o}(\vec{q}) \exp[2R(\vec{q})t]. \tag{32}$$

where the prefactor $S_{T_o}(\vec{q})$ simply is the equal-time structure factor in thermal equilibrium at the temperature T_o before the quench,

$$S_{T_o}(\vec{q}) \equiv \langle \delta c_{-\vec{q}}(0) \delta c_{\vec{q}}(0) \rangle_T = \langle \delta c_{-\vec{q}} \delta c_{+\vec{q}} \rangle_{T_o}. \tag{33}$$

Note that $R(\vec{q})$ is positive for $0 < q < q_c$, with $R(q) = k_B T M q^2 r^2 (q_c^2 - q^2)/d$, and

$$q_c = \frac{2\pi}{\lambda_c} = [-d(\partial^2 f_{cg}/\partial c^2)_{T, c=\bar{c}}/(r^2 k_B T)]^{1/2}. \tag{34}$$

Using equation (9), as an example, we obtain

$$(\partial^2 f_{cg}/\partial c^2)_{T,c=\bar{c}} = A c_{crit}^{-2} + 3B c_{crit}^{-4} (\bar{c} - c_{crit})^2 = c_{crit}^{-4} B [3(\bar{c} - c_{crit})^2 - (c_{coex} - c_{crit})^2] < 0 \quad \text{if } |\bar{c} - c| < |c_{sp} - c_{crit}| = |c_{coex} - c_{crit}|/\sqrt{3}.$$

This is the behavior anticipated in Figure 1.

As a next step, we discuss the effect of statistical fluctuations in the framework of the linearized theory [3, 5, 129]. Equations (23)–(25) can be cast into the form

$$\frac{d}{dt} S(\vec{q}, t) = -2M k_B T q^2 \{ [\partial^2 f_{cg}/\partial c^2)_{T,c=\bar{c}}/k_B T + r^2 q^2/d] S(\vec{q}, t) - 1 \}. \tag{35}$$

Equation (35) is useful for describing relaxation phenomena in the stable and metastable region of the phase diagram, where $(\partial^2 f_{cg}/\partial c^2)_{T,c=\bar{c}} > 0$ and $S(\vec{q}, t \to \infty)$ tends to an equilibrium structure factor of Ornstein-Zernike form

$$S_T(\vec{q}) = [(\partial^2 f_{cg}/\partial c^2)_{T,c=\bar{c}}/k_B T]^{-1}/(1 + q^2 \xi_b^2), \tag{36}$$

where $\xi_b = r/\sqrt{d(\partial^2 f_{cg}/\partial c^2)_{T,c=\bar{c}}/k_B T}$ is the correlation length of concentration fluctuations {at the coexistence curve this expression reduces to equation (20), of course, if equation (9) is invoked}. Then equation (35) simply leads to an exponential relaxation

from one Ornstein-Zernike structure factor $S_{T_o}(\vec{q})$ in the initial state to the other,

$$S(\vec{q}, t) = S_{T_o}(\vec{q}) \exp[2R(q)t] + S_T(\vec{q}) \{1 - \exp[2R(\vec{q})t]\}, \tag{37}$$

since $R(\vec{q})$ then is negative. Inside of the spinodal curve, where $R(\vec{q})$ is positive, equation (37) still is a solution of equation (35) if $S_T(\vec{q})$ is re-interpreted as the so-called "virtual structure factor" $S_T(\vec{q}) = [(\partial^2 f_{cg}/\partial c^2)_{T,c=\bar{c}}/k_B T]^{-1}/(1 - q^2/q_c^2)$, which clearly is singular at q_c. However, neither this singularity nor the exponential growth of the initial fluctuations (described by $S_{T_o}(q)$) are physically meaningful, since the nonlinear terms eliminate this pathological behavior completely. Thus a well-defined critical wavenumber q_c does not exist, apart from the case of long range interactions ($r \to \infty$) [14, 15]. This last remark can be verified from an extension of the Ginzburg criterion [133], a selfconsistency criterion for the accuracy of mean field theory, to spinodal decomposition [14]. One argues that the linear theory presented in Equations (27)–(37) is valid if the meansquare amplitude of concentration fluctuations in a coarse-graining cell of linear dimension L is small in comparison with the concentration difference squares in the system over which relevant nonlinear effects are felt,

$$\langle [\delta c(\vec{x}, t)]^2 \rangle_{T,L} < < [\bar{c} - c_{sp}(T)]^2 \tag{38}$$

{remember that $(\partial^2 f_{cg}/\partial c^2)_T$ changes sign at the spinodal, we have $(\partial^2 f_{cg}/\partial c^2)_T \approx 6 c_{crit}^{-4} B(\bar{c} - c_{sp}(T))(c_{sp}(T) - c_{crit})$}. Now we estimate $\langle [\delta c(\vec{x}, t)]^2 \rangle_{T,L}$ as

$$\langle [\delta c(\vec{x}, t)]^2 \rangle_{T,L} \approx \langle [\delta c(\vec{x}, 0)]^2 \rangle_{T,L} \exp[2R(q_m)t], \tag{39}$$

$q_m = q_c/\sqrt{2}$ being the wavenumber where the growth rate $R(q)$ (eq. (31)) is maximal. Now for $L < \xi_b$ the factor $\langle [\delta c(\vec{x}, 0)]^2 \rangle_{T,L}$ is estimated [14] to be of the order of $a^3 r^{-2} L^{-1}$, and taking the maximum self-consistent choice for L, which is $L \approx \lambda_c$, one obtains that equation (38) is equivalent to (in $d = 3$ dimensions)

$$\exp[2R(q_m)t] < < (r/a)^3 (1 - T/T_{cb})^{1/2} [\bar{c}/c_{sp}(T) - 1]^{3/2}, \tag{40}$$

a being the interatomic distance. Obviously, equation (40) can be satisfied at all only if $r/a > > 1$, since the other factors on the right hand side are less than unity. Even then the range of times over which exponential growth of fluctuations (with negligible coarsening behavior) occurs is rather restricted: the time where nonlinear effects set in (to be estimated roughly from equation (40) by reading this equation as an equality rather than an inequality) increases only with ln r. Conversely, for short range systems nonlinear effects are present already in the very early stages of phase separation, and equations (27)–(37) do not have a quantitative validity at all, though they still yield qualitatively reasonable predictions for the initial growth rate $R(q, t = 0)$ and the scale of q_m where initially maximum growth occurs [134].

3. Surface effects on spinodal decomposition: Linear analysis

We now consider first semi-infinite geometry, assuming that the mixture can exist only for $Z > 0$, and is bound by a hard wall at $Z = 0$, and hence in our (rescaled) coordinate

$\vec{X}$ (eq. (20)) we distinguish coordinates parallel ($\vec{R}$) and perpendicular (Z) to this wall, $\vec{X} \equiv (\vec{R}, Z)$. Now an obvious constraint is that there cannot be any concentration current across the wall, i.e. $j_z(\vec{X}, t) = -M\partial\mu(\vec{X}, t)/\partial z|_{z=0} = 0$, which then yields (taking steps analogous to eq. (15)–(19)) [70]

$$\frac{\partial}{\partial Z}[\phi(\vec{R}, Z, \tau) - \phi^3(\vec{R}, Z, \tau) + \frac{1}{2}\nabla^2\phi(\vec{R}, Z, \tau)]_{z=0} = 0 \tag{41}$$

However, equation (41) is not the only boundary condition that is needed: this is clear both from mathematical reasons (eq. (41) would not fix the solution of eq. (19) uniquely [135]) and from physical arguments: one expects that a wall exerts preferential forces on one species of the mixture relative to the other species, there may also occur a change of pairwise forces among the particles that are close to the wall, etc. [51]. Assuming that all these direct effects of the wall on the mixture are of short range, one is led to the following boundary condition [67, 70, 82, 101]

$$\frac{\partial\phi(\vec{R}, 0, \tau)}{\partial\tau} = h_1 + g\phi(\vec{R}, 0, \tau) + \gamma\frac{\partial\phi(\vec{R}, Z, \tau)}{\partial Z}|_{z=0} + \frac{1}{2}\gamma'\nabla_R^2\phi(\vec{R}, 0, \tau) \tag{42}$$

where h_1, g, γ and γ' are phenomenological parameters which we will discuss below. Equation (42) clearly has the effect that the order parameter right at the surface rapidly relaxes to an equilibrium value dictated by the competition between the "surface field" h_1 and the energy cost involved in order parameter gradients. Equation (42) can also be derived by requiring that the system minimizes in thermal equilibrium also its surface free energy, while Equation (19) leads to minimization of the bulk free energy.

While boundary conditions such as equations (41), (42) can be derived from fairly general considerations involving mostly symmetry principles [136], we follow here a rather straightforward approach [67, 82] based on the consideration of a lattice model for an alloy with a free surface (Fig. 7). We assume for the moment pairwise interactions $\varphi_{AA}(\vec{x}_i, \vec{x}_j)$, $\varphi_{AB}(\vec{x}_i, \vec{x}_j)$ and $\varphi_{BB}(\vec{x}_i, \vec{x}_j)$ between atoms at sites $\vec{x}_i$, $\vec{x}_j$. In terms of local concentration variables $\{c_i = 1$ if site i is occupied by an A-atom, $c_i = 0$ if it is occupied by a B atom$\}$ the Hamiltonian of the system can then be written

$$\begin{aligned}\mathcal{H} = \sum_{i\neq j}[&c_i c_j \varphi_{AA}(\vec{x}_i, \vec{x}_j) + c_i(1-c_j)\varphi_{AB}(\vec{x}_i, \vec{x}_j) \\ &+ (1-c_i)c_j\varphi_{AB}(\vec{x}_i, \vec{x}_j) + (1-c_i)(1-c_j)\varphi_{BB}(\vec{x}_i, \vec{x}_j)] \\ &+ \sum_i [v_A(\vec{x}_i)c_i + v_B(\vec{x}_i)(1-c_i)]\end{aligned} \tag{43}$$

Here it is assumed that sums over pairs run over all pairs once, lattice sites exist in the positive half space $Z > 0$ only, and $v_A(\vec{x}_i)$ $[v_B(\vec{x}_i)]$ are forces exerted on $A(B)$ atoms at site $\vec{x}_i$ due to the hard wall. In the following, we assume that these forces act in the first layer adjacent to the wall ($n = 1$) only, although the generalization to the case of long range surface forces sometimes is necessary [55]. Similarly, although one must expect that the surface breaks the translational symmetry of the system, and hence pairwise

interactions can depend on both sites $\vec{x}_i$, $\vec{x}_j$ separately and not just on their distance $\vec{x}_i - \vec{x}_j$ only, we assume that all (nearest neighbor) interactions φ_{AA}, φ_{BB}, φ_{AB} throughout the system are the same, apart from the surface plane ($n = 1$) where we assume different interactions that we denote as φ^s_{AA}, φ^s_{AB} and φ^s_{BB}, if both sites $\vec{x}_i$, $\vec{x}_j$ are in the layer $n = 1$.

Of course, Figure 7 is not meant as a "correct" description of atomistic detail, but rather serves as a generic model to derive a reasonable continuum description that holds then for a much larger class of systems. The first step is the translation of equation (43) to the Ising pseudo-spin representation [51] via the transformation $c_i = (1 - S_i)/2$, with $S_i = \pm 1$. In terms of the chemical potentials μ_A, μ_B of both species, this yields

$$\mathcal{H} - \sum_i c_i\mu_A - \sum_i (1-c_i)\mu_B = -\sum_{i,j} J_{ij}S_iS_j - H\sum_i S_i - H_1\sum_{i\in 1^{st}\text{layer}} S_i + \mathcal{H}_0 \tag{44}$$

where $\mathcal{H}_0$ is a constant that only affects the energy scale, and hence is omitted. The pairwise "exchange" energy J_{ij} is

$$J_{ij} = J = \frac{1}{2}\varphi_{AB} - \frac{1}{4}(\varphi_{AA} + \varphi_{BB}), \tag{45}$$

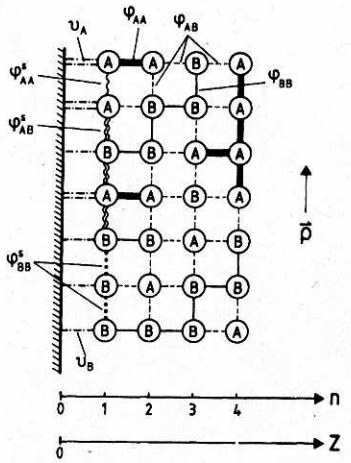

Fig. 7: Schematic picture of the surface of a binary (AB) alloy at $Z = 0$ (the shading indicates that this may represent an inert hard wall). Different atoms (circles) and nearest-neighbor interactions between them (and the wall) are indicated by different types of lines. For a discrete description, lattice planes parallel to the surface are labeled by a positive integer n, while in the continuum description coordinates parallel ($\vec{\rho}$) and perpendicular (z) to the surface are used as indicated. From Puri and Binder [82].

when at least one of the sites i, j is not in the surface layer, $n = 1$. If both sites are in the surface layer, we have

$$J_{ij} = J_s = \frac{1}{2}\varphi^s_{AB} - \frac{1}{4}(\varphi^s_{AA} + \varphi^s_{BB}) \tag{46}$$

The bulk "magnetic field" H is (for sites i not in the $n = 1$ layer)

$$H = \frac{1}{2}(\mu_B - \mu_A) + \frac{1}{2}\sum_{j(\neq i)} (\varphi_{AA} - \varphi_{BB}), \tag{47}$$

while for sites i in the first layer we have an additional "surface field" H_1,

$$H + H_1 = \frac{1}{2}(\mu_B - \mu_A + v_B - v_A) + \frac{1}{2}\Big[\sum_{j\in 1^{st}\text{layer}} (\varphi^s_{AA} - \varphi^s_{BB}) + \sum_{j\in 2^{nd}\text{layer}} (\varphi_{AA} - \varphi_{BB})\Big]. \tag{48}$$

A nonzero surface field arises even for the case where $v_B = v_A = 0$ and interactions are unchanged near the surface, i.e. $\varphi^s_{AA} = \varphi_{AA}$ and $\varphi^s_{BB} = \varphi_{BB}$, as long as $\varphi_{AA} - \varphi_{BB} \neq 0$. This is a consequence of the "missing neighbours" of sites in the first layer.

The "bulk field" H in equation (44) is eliminated from the problem by fixing the average concentration

$$\bar{c} = (1/N)\sum_i \langle c_i \rangle, \tag{49}$$

which also is the concentration c_b in the bulk of this semi-infinite system. But the additional surface field H_1 remains as a parameter in the problem; as is well-known [51, 55], this term is responsible for surface enrichment and wetting phenomena in mixtures.

We now associate dynamics to equation (44) via the spin exchange Kawasaki model [131], allowing direct exchanges between nearest neighbours on the lattice. Again this is not meant as a realistic description of solid alloys (which would require to consider a vacancy mechanism of diffusion [137]), but serves to motivate the coarse-grained continuum model. One obtains a set of coupled kinetic equations for the local time-dependent mean magnetization on a lattice site, $\langle S_i(t)\rangle \equiv m_n(\vec{\rho}, t)$, treating the (exact) master equation [131] in mean field approximation [125]. As an example, we quote here the equation for the surface layer [67] (τ_s is a constant setting the time scales for the attempted spin exchanges, q is the coordination number)

$$2\tau_s \frac{d}{dt} m_1(\vec{\rho}, t) = -(q-1)m_1(\vec{\rho}, t) + m_2(\vec{\rho}, t) + \sum_{\Delta\vec{\rho}} m_1(\vec{\rho} + \Delta\vec{\rho}, t) + [1 - m_1(\vec{\rho}, t)m_2(\vec{\rho}, t)]\tanh\frac{J}{k_B T}\Big[m_2(\vec{\rho}, t) + H_1/J + \frac{J_s}{J}\sum_{\Delta\vec{\rho}} m_1(\vec{\rho} + \Delta\vec{\rho}, t) - m_3(\vec{\rho}, t) - m_1(\vec{\rho}, t)$$

$$-\sum_{\Delta\vec{\rho}} m_2(\vec{\rho} + \Delta\vec{\rho}, t)\Big] + \sum_{\Delta\vec{\rho}} [1 - m_1(\vec{\rho}, t)m_1(\vec{\rho} + \Delta\vec{\rho}, t)]\tanh\frac{J}{k_B T} \times \Big[m_2(\vec{\rho}, t) + \frac{J_s}{J}\sum_{\Delta\vec{\rho}'} m_1(\vec{\rho} + \Delta\vec{\rho}', t) - m_2(\vec{\rho} + \Delta\vec{\rho}, t) - \frac{J_s}{J}\sum_{\Delta\vec{\rho}'} m_1(\vec{\rho} + \Delta\vec{\rho}' + \Delta\vec{\rho}, t)\Big] \tag{50}$$

Here $\Delta\vec{\rho}$ is a vector connecting site i with one of its $q-2$ nearest neighbours in a layer. Obviously, equation (50) is rather clumsy, and so are the kinetic equations for the local magnetizations in the second and further layers [67], which hence are not reproduced here. Still, when one linearizes these equations in the $m_n(\vec{\rho}, t)$, one still can find the solutions of this coupled set of equations exactly. E.g., in the case where no inhomogeneity in lateral direction is considered, i.e. $m_n(\vec{\rho}, t)$ simply can be written as $m_n(t)$, one can easily find the Laplace transform $\bar{m}_n(s)$,

$$\bar{m}_n(s) = \int_0^\infty \exp(-st)[m_n(t) - m_b]dt, \tag{51}$$

m_b being the equilibrium magnetization in the bulk. For states in the one-phase region of the mixture the result is [67]

$$\bar{m}_n(s) = B_+(s)\exp[-n/\xi_+(s)] + B_-(s)\exp[-n/\xi_-(s)], \tag{52}$$

where the amplitudes $B_+(s), B_-(s)$ are expressed in terms of the boundary conditions at the surface, and $\xi_\pm(s)$ are effective frequency-dependent correlation lengths given by the equation [67]

$$\sinh[1/2\xi_\pm(s)] = \frac{1}{2}\Big\{-\frac{q}{2}\Big(1 - \frac{T}{T_c}\Big) \pm [q(1 - T/T_c)^2 - 2\tau_s k_B Ts/J]^{1/2}\Big\}^{1/2}. \tag{53}$$

For low frequency, $s \to 0$ {i.e., large times} the smaller length $\xi_-(s)$ converges to the correlation length $\xi_b = \frac{1}{\sqrt{q}}\Big(\frac{T}{T_{cb}} - 1\Big)^{-1/2}$, choosing the lattice spacing as unity, while the larger length behaves as

$$\xi_+(s) \approx (2\tau_s T/T_c)^{-1/2}[s/(T/T_c - 1)]^{-1/2}. \tag{54}$$

This result shows that at large times t the order parameter profile $m_n(t)$ exhibits structure at a "diffusion length" $\xi_+(1/t) \propto [t(T/T_c - 1)]^{-1/2}$, as one might have naively expected: the surface excess concentration required by the boundary conditions is transported from the bulk to the surface via diffusion, creating a shallow "depletion zone" which spreads out more and more as time passes after the quench (remember that eqs. (51)–(54) refer to a quench in Figure 1 where both initial and final temperatures T_o, T are still in the one-phase region).

Apart from the possibility to solve equations such as equation (50) directly, one can use them to derive boundary conditions to the Cahn-Hilliard equation [67]. This is done by transforming from differences to differentials, e.g.

$$m_n(\vec{\rho}+\Delta\vec{\rho},t)=m_n(\vec{\rho},t)+(\Delta\rho\cdot\vec{\nabla}_\parallel)m_n(\vec{\rho},t)+\frac{1}{2}(\Delta\rho\cdot\nabla_\parallel)^2 m_n(\vec{\rho},t)$$
$$+\frac{1}{6}(\Delta\rho\cdot\vec{\nabla}_\parallel)^3 m_n(\vec{\rho},t)+\frac{1}{24}(\Delta\rho\cdot\vec{\nabla}_\parallel)^4 m_n(\vec{\rho},t), \tag{55}$$

and similarly the discrete index n is transformed to a continuous coordinate z. In this way one derives as an equation in the bulk a special case of equation (18), namely

$$2\tau_s\frac{\partial}{\partial t}m(\vec{\rho},z,t)=\nabla^2\left\{\left(1-\frac{T_c}{T}\right)m+\frac{1}{3}m^3-\frac{1}{q}\nabla^2 m\right\}, \tag{56}$$

and the nontrivial boundary condition (equivalent to Eq. (42)) becomes [67]

$$2\tau_s\frac{\partial}{\partial t}m(\vec{\rho},0,t)=\frac{H_1}{k_B T}+\left[\frac{J_s(q-2)-(q-1)J}{k_B T}\right]m(\vec{\rho},0,t)$$
$$+\left[1-\frac{(q-1)J}{k_B T}\right]\frac{\partial m(\vec{\rho}),z,t}{\partial z}|_{z=0}$$
$$+\frac{1}{2}\left\{1-\left[\frac{J_s}{k_B T}(q-3)+\frac{2J}{k_B T}\right]\right\}\sum_{\Delta\vec{\rho}}(\Delta\vec{\rho}\cdot\nabla_\parallel)^2 m(\vec{\rho},0,t)+\cdots \tag{57}$$

where we kept only the same lowest order terms as written in equation (42) (see Ref.[67] for a derivation of higher order corrections). Thus indeed h_1 is a (suitably rescaled) surface magnetic field, in the Ising spin notation, g can be related to the change of interactions in the surface layer, etc.

We now discuss surface effects on spinodal decomposition in the framework of the linearized theory, using in equation (19) $\phi^3(\vec{R},Z,\tau)\approx\phi_0^3+3\phi_0^2\delta\phi(\vec{R},Z,\tau)$ so that the bulk equation becomes

$$\frac{\partial}{\partial\tau}\delta\phi(\vec{R},Z,\tau)=-\nabla^2(1-3\phi_0^2+\frac{1}{2}\nabla^2)\delta\phi(\vec{R},Z,\tau), \tag{58}$$

while the no-flux boundary condition becomes

$$\frac{\partial}{\partial Z}\left[1-3\phi_0^2+\frac{1}{2}\nabla^2\right]\delta\phi(\vec{R},Z,\tau)|_{Z=0}=0, \tag{59}$$

which has to be treated together with equation (42). Using Fourier transforms with respect to the lateral coordinate $\vec{R}$,

$$\delta\phi_{k_\parallel}(Z,\tau)=\int d\vec{R}\exp(i\vec{k}_\parallel\cdot\vec{R})\delta\phi(\vec{R},Z,\tau) \tag{60}$$

yields a set of equations

$$\frac{\partial}{\partial\tau}\delta\phi_{k_\parallel}(Z,\tau)=\left(k_\parallel^2-\frac{\partial^2}{\partial Z^2}\right)\left(1-3\phi_0^2-\frac{1}{2}k_\parallel^2+\frac{1}{2}\frac{\partial^2}{\partial Z^2}\right)\delta\phi_{k_\parallel}(Z,\tau), \tag{61}$$

$$\frac{\partial}{\partial Z}\left\{\left[1-3\phi_0^2-\frac{1}{2}\left(k_\parallel^2-\frac{\partial^2}{\partial Z^2}\right)\right]\delta\phi_{k_\parallel}(Z,\tau)\right\}|_{Z=0}=0, \tag{62}$$

$$\frac{\partial}{\partial\tau}\delta\phi_{k_\parallel}(0,\tau)=h_1\delta_{k_\parallel 0}+g\delta\phi_{k_\parallel}(0,\tau)+\gamma\frac{\partial}{\partial Z}\delta\phi_{k_\parallel}(Z,\tau)|_{Z=0}$$
$$-\frac{1}{2}\gamma' k_\parallel^2\delta\phi_\parallel(0,\tau). \tag{63}$$

Note that although Puri and Binder [82] and Frisch *et al.* [96] included higher order terms $\partial^2\delta\phi_{k_\parallel}(Z,\tau)/\partial Z^2|_{Z=0}$ etc. in their treatment, they igonred the last term $-\frac{1}{2}\gamma' k_\parallel^2\delta\phi_\parallel(0,\tau)$, although the microscopic theory [67] clearly shows that it is present (see the term involving $\nabla_\parallel^2$ in equation (57)). As pointed out by Fischer *et al.* [101], this term is crucial to obtain the dispersion relation for the lateral surface modes. Equations (61)–(63) represent an inhomogeneous boundary value problem, with the inhomogeneity appearing only for $k_\parallel=0$.

We discuss briefly the solution of equations (61)–(63) next. The general solution can be constructed as a superposition of a special solution of the inhomogeneous problem, present for $k_\parallel=0$, and of the general solution of the homogeneous problem. The latter is solved attempting a solution

$$\delta\phi_{k_\parallel}(Z,\tau)=\exp(wt)\sum_j a_j e^{-K_j Z}, \tag{64}$$

which implies for K_j the condition

$$K_j^2=k_\parallel^2-k_m^2\pm i\sqrt{2w-k_m^4}, \tag{65}$$

where $k_m=\sqrt{1-3\phi_0^2}$ is the wavenumber of maximal growth of the bulk modes. Physically sensible solutions require $a_j=0$ if $Re K_j<0$, and thus only two out of the four solutions of equation (65) are meaningful. The boundary conditions equations (62)–(63) then yield a homogeneous system of two linear equations for the remaining amplitude a_j. The condition that this system has a nontrivial solution then yields the spectrum of allowed modes [101], $w=w_s(k_\parallel)$. It should be noted, however, that the observability of such surface modes in general will be restricted to extremely short times, since the mode $\delta\phi_{k_\parallel=0}(Z,\tau)$ relaxes much faster and thus the homogeneous

initial condition assumed in the linearized theory disappears near the surface, the nonlinear interactions between the surface modes, equation (64), and the mode $\delta\phi_{k_\parallel=0}(Z, 0)$ need to be considered. Using again Laplace transforms

$$\bar{u}(Z, s) = \frac{1}{2}\int_0^\infty \exp(-s\tau/2)\delta\phi_{k_\parallel=0}(Z, \tau)\, d\tau \tag{66}$$

Equation (61) leads to the following equation ($u_0(Z) = \delta\phi_{k_\parallel=0}(Z, 0)$ is the initial condition)

$$s\bar{u} - u_0 = -2k_m^2 \partial^2\bar{u}/\partial Z^2 - \partial^4\bar{u}/\partial Z^4, \tag{67}$$

with the boundary conditions resulting from equations (62), (63)

$$2k_m^2 \partial\bar{u}(Z, s)/\partial Z|_{Z=0} + \partial^3\bar{u}(Z, s)/\partial Z^3|_{Z=0} = 0 \tag{68}$$

$$s\bar{u}(0, s) - u_0(0) = h_1/2s + \frac{g}{2}\bar{u}(0, s) + \frac{\gamma}{2}\frac{\partial\bar{u}(Z, s)}{\partial Z}|_{Z=0} \tag{69}$$

which is solved by [96, 138]

$$\bar{u}(Z, s) = u_0/s + C(s)e^{-\nu(s)Z}\cos[\mu(s)Z - \varphi(s)] \tag{70}$$

where the inverse characteristic lengths $\mu(s)$, $\nu(s)$ are the solutions of the following equations

$$\mu^2(s) = \frac{1}{6}(4k_m^2 \pm \sqrt{2}\sqrt{3s - k_m^4}), \tag{71}$$

$$\nu^2(s) = \frac{1}{6}(-2k_m^2 \pm \sqrt{2}\sqrt{3s - k_m^4}), \tag{72}$$

where $s \geqslant s_0 = k_m^4$ is needed to ensure that both $\nu^2(s)$ and $\mu^2(s)$ are non-negative. For $s = s_0$ we have $\nu^2(s_0) = 0$ while $\mu^2(s_0) = k_m^2$. This finding implies that the characteristic wavelength of spinodal decomposition in the bulk determines also the scale of the order parameter at the surface. While the phase $\varphi(s)$ in equation (70) can also be found in terms of $\mu(s)$ and $\nu(s)$, the amplitude $C(s)$ then carries the information on the parameters h_1, g and γ due to the boundary condition, equation (69), [96]. Figure 8 shows typical results for the surface part $V(Z, s) \equiv \bar{u}(Z, s) - u_0/s$ obtained from this treatment. Since the zeros of $V(Z, s)$ are approximately independent of s, it is plausible that $\delta\phi_{k_\parallel=0}(Z, \tau)$ also shows zeros at a distance $\lambda_m = 2\pi/k_m$ as is obvious from the numerical solution of the full nonlinear problem (Fig. 9).

4. Numerical results for surface-directed spinodal decomposition in the framework of a nonlinear theory

While the rapid relaxation of $\phi(\vec{R}, Z, \tau)$ near the wall at $Z = 0$ enforced by the boundary condition, equation (42), stabilizes surface-directed concentration waves with a

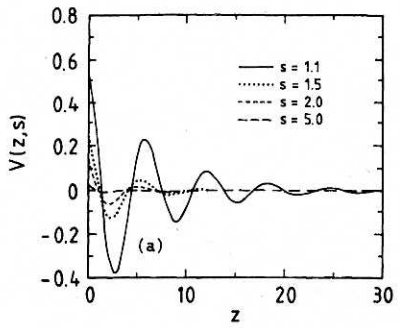

Fig. 8: Surface part $V(Z, s) = \bar{u}(Z, s) - u_0/s$ of the Laplace transform, Eq. (70), plotted vs. the scaled distance Z for the choice of parameters $u_0 = 0.025$, $\phi_0 = 0$, $h_1 = 4$, $\gamma = 4$ and $g = -4$, i.e. a system where in equilibrium there is considerable surface enrichment, but the surface still is nonwet. Four values of the scaled frequency s are shown, as indicated in the figure. From Frisch *et al.* [96]

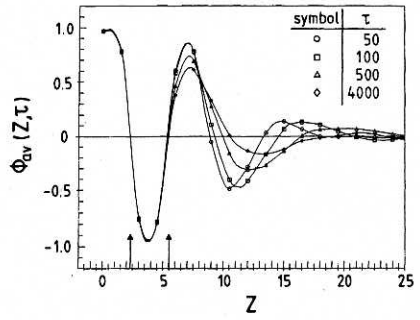

Fig. 9: Averaged profiles $\phi_{av}(Z, \tau)$ as a function of the scaled distance Z from the surface, for four scaled times τ as indicated. Data were obtained from a discrete implementation of Eqs. (19), (41), (42) for the choice of parameters $h_1 = 4, g = -4, \gamma = 4, \gamma' = 0$, using a lattice of size 150×300, and an initial condition with uniformly distributed random fluctuations of amplitudes ± 0.025 about a zero background, corresponding to a critical quench ($\phi_0 = 0$) from infinite temperature ($T_0 \to \infty$ in Fig. 1). Averaging is done laterally (in the X-direction parallel to the surface) and over an ensemble of fifty independent initial conditions. Arrows indicate the predictions of the linear theory for the first two zeros of $\phi_{av}(Z, \tau)$, namely $k_m Z_0^{(n)} = \pi/4 + (2n + 1)\pi/2$, $n = 0, 1, \ldots$. Numerical results were taken from Puri and Binder [82]. From Frisch *et al.* [96]

wavevector oriented along the z-axis, it is clear that the large amplitudes of these concentration waves invalidate the linearized treatment of the previous section, nonlinear effects will give rise to a coarsening as in the bulk (Sect. 2). However, since the directions parallel and perpendicular to the walls are non-equivalent, it clearly is of interest to consider not only the bulk length scale $\lambda_m(t)$ used to describe the coarsening

in the bulk, equation (1), but to introduce length scales $l_\parallel(Z,\tau)$, $l_\perp(Z,\tau)$ characterizing the growth of concentration fluctuations in the directions parallel and perpendicular to the surface (due to the fact that the wall breaks the translational invariance in the z-direction, these length scales may in fact depend on Z but for $Z\to\infty$ we expect $l_\parallel(Z,\tau)=l_\perp(Z,\tau)=l_b(\tau)$, the suitably rescaled bulk length scale $\lambda_m(t)$).

In order to give these length scales $l_\parallel(Z,\tau)$, $l_\perp(Z,\tau)$ a precise meaning, it is convenient to introduce the order parameter correlation function [82]

$$G(\vec{R}_1-\vec{R}_2,Z_1,Z_2,\tau)=\langle\phi(\vec{R}_1,Z_1,\tau)\phi\,\vec{R}_2,Z_2,\tau)\rangle - \langle\phi(\vec{R}_1,Z_1,\tau)\rangle\langle\phi(\vec{R}_2,Z_2,\tau)\rangle, \tag{73}$$

where our notation already indicates translational invariance in the directions parallel to the wall only. Writing as an abbreviation (the overbar means a spherical average over the direction of $\vec{R}_1-\vec{R}_2$)

$$G_\parallel(|\vec{R}_1-\vec{R}_2|,Z,\tau)\equiv\bar{G}(\vec{R}_1-\vec{R}_2,Z,Z,\tau), \tag{74}$$

a practically convenient definition of $L_\parallel(Z,\tau)$ is then the distance over which $G_\parallel$ has decayed to half its maximum value [82],

$$G_\parallel(l_\parallel(Z,\tau),Z,\tau)=G_\parallel(0,Z,\tau)/2. \tag{75}$$

A perpendicular length scale is defined similarly, i.e. [82]

$$G(0,Z,Z+l_\perp(Z,\tau),\tau)=G(0,Z,Z,\tau)/2. \tag{76}$$

A nontrivial behavior of these length scales is to be expected particular in cases where an interplay between the growth of wetting layers at the surfaces and spinodal decomposition in the bulk occurs [82, 100]. In Figure 10 we briefly recall the basic aspects of wetting phenomena for binary fluid mixtures in thermal equilibrium [54, 55, 56] denoting for the moment the volume fraction of species A (that is not attracted to the walls) as ϕ_b in the bulk. Then wetting is described in terms of the surface excess

$$\phi_s=\int_0^\infty dZ\,[\phi_b-\phi(Z)] \tag{77}$$

as one approaches phase coexistence at the B-rich side of the coexistence curve, $\phi^{(2)}_{coex}$. If ϕ_s is considered as a function of ϕ_b at constant T, one can distinguish between incomplete wetting (if $\phi_s^{(2)}=\phi_s(\phi_b\to\phi^{(2)}_{coex})$ is finite) or complete wetting ($\phi_s^{(2)}\to\infty$, due to the adsorption of a macroscopically thick B-rich enrichment layer at the wall). At a temperature T_w, or alternatively an inverse interaction parameter χ_w^{-1}, we have a wetting transition between a nonwet and a wet state, which can either be of first order (as assumed in Fig. 10a) or of second order.

Now the boundary condition, equation (42), has been deliberately chosen such that it can describe conditions of both wet and nonwet surfaces, and the full phase diagram of

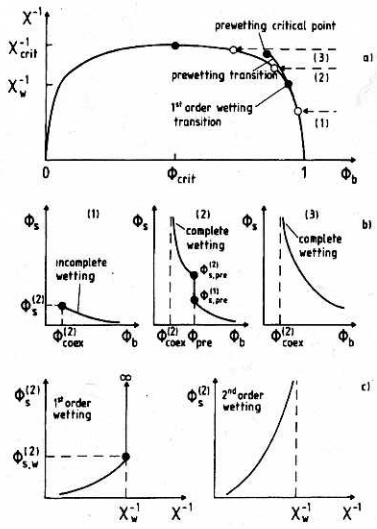

Fig 10: (a) Schematic phase diagram of a semi-finite mixture exhibiting a first-order wetting transition on the A-rich side of the coexistence curve for an interaction parameter $\chi=\chi_w$. In this case there exists a prewetting transition line in the A-rich one phase region, beginning at the 1st order wetting transition at the coexistence curve and ending in a prewetting critical point. Three paths (1), (2), (3) are indicated in the one-phase region, where one approaches the coexistence curve at constant χ by reducing the bulk volume fraction ϕ_b of the mixture. (b) Variation of the surface excess ϕ_s plotted vs. ϕ_b for the three paths (1), (2), (3). For $\chi^{-1}<\chi_w^{-1}$ and $\phi_b\to\phi^{(2)}_{coex}$ the surface excess reaches a finite limit $\phi^{(2)}$ ("incomplete wetting"), while for $\chi^{-1}>\chi_w^{-1}$ the surface excess diverges at phase coexistence ("complete wetting"). For $\phi=\phi_{pre}$ a finite jump of ϕ_s from $\phi^{(1)}_{s,pre}$ to $\phi^{(2)}_{s,pre}$ occurs ("1st order prewetting transition"). This jump $\phi^{(2)}_{s,pre}$ smoothly vanishes as the prewetting critical point is reached. (c) Variation of $\phi_s^{(2)}$ with χ^{-1} at phase coexistence {i.e., ϕ_b is kept at $\phi^{(2)}_{coex}(\chi)$}. At the first order wetting transition, $\phi_s^{(2)}$ jumps from a finite value $\phi^{(2)}_{s,w}$ discontinuously to infinity, while a critical divergence of $\phi_s^{(2)}$ is encountered for the 2nd order wetting transition.

Figure 10 is reproduced. In fact, the free energy functional that describes the thermal equilibrium associated with equations (19), (41) and (42) is [139]

$$\frac{\Delta\mathcal{F}}{k_BT_c}=\int d\vec{R}\left\{\int_0^\infty dZ\frac{1}{2}\left[\frac{1}{2}(\nabla\phi)^2-\phi^2+\frac{1}{2}\phi^4\right]-\frac{h_1}{\gamma}\phi_1-\frac{1}{2}\frac{g}{\gamma}\phi_1^2\right\} \tag{78}$$

where $\phi_1(\vec{R})\equiv\phi(\vec{R},Z=0)$ is the local order parameter at the surface. As is well-known, the thermal equilibrium profile $\phi_{eq}(Z)$ results from minimizing this free energy functional, which yields an Euler-Lagrange equation

$$\phi_{eq}(Z)-\phi_{eq}^3(Z)+\frac{1}{2}\partial^2\phi_{eq}(Z)/\partial Z^2=0, \tag{79}$$

with the boundary condition

$$h_1 + g\phi_{eq}(Z=0) + \gamma\partial\phi_{eq}(Z)/\partial Z|_{Z=0} = 0. \tag{80}$$

Obviously, if we look for a time-independant, stationary solution of equations (19), (41) and (42), putting all time-derivatives equal to zero and seeking a solution that is homogeneous in lateral directions, we recover equation (79) from equation (19), and equation (80) from equation (41).

The surface phase diagram that results from equations (78)–(80) has been discussed previously in detail [139]. Here we only note that a second-order wetting transition occurs for $g/\gamma < -2$, at a critical value of the surface field given by $h_1 = h_{1c}(g,\gamma) = -g$, while for $g/\gamma > -2$ the wetting transition is of first order. In this regime the transition line $h_{1c}(g,\gamma)$ needs to be calculated numerically (it lies in between the spinodal of the wet surface phase, which is $h_{1s}^{(1)}(g,\gamma) = -g$, and the spinodal of the non-wet surface phase, which is $h_{1s}^{(2)}(g,\gamma) = \gamma + g^2/(4\gamma)$). For $h_1 < h_{1c}(g,\gamma)$ the surface is not-wet (or incompletely wet, respectively), while for $h_1 > h_{1c}(g,\gamma)$ it is wet. It is interesting to recall what this means in terms of the profiles that result from equation (79): the solutions admitted by equation (79) are the functions $\phi'(Z) = \pm\tanh(Z - Z_0)$ and $\phi''(Z) = \pm\coth(Z - Z_0)$. In the incompletely wet case it is only $\phi'(Z)$ that contributes; the constant Z_0 is adjusted such that equation (80) is satisfied, which gives $\phi_1 = g/(2\gamma) \pm \sqrt{(g/2\gamma)^2 + 1 + h_1/\gamma}$. Choosing the sign such that $\phi'(Z\to\infty) = -1$, we note that for $h_1 \to h_{1c}$ we obtain $\phi_1 \to 1$, $Z_0 \to \infty$, i.e. the interface "unbinds" from the walls, as expected for a wetting phenomena. In the wet case, the near-surface part of the profile utilizes $\phi''(Z)$, on the other hand, one first has a decay from a value $\phi_1 > 1$ to $\phi_1 = 1$ as $Z \to \infty$, and then a decay from $\phi = +1$ to $\phi = -1$ via a $-\tanh(Z - Z_0)$ profile occurs for $Z_0 \to \infty$ (macroscopically thick wetting layer).

This behavior of the surface enrichment profiles $\phi_{eq}(Z)$ in equilibrium has its counterpart in the profiles $\phi_{av}(Z,\tau)$ that result from the numerical solution of equations (19), (41) and (42) (here the subscript "av" stands for a lateral average over the coordinate $\vec{R}$ in a system which is 300 length units long in lateral direction, applying periodic boundary conditions, and for an average over 50 individual runs). Figure 11 gives an example both for an incompletely wet situation ($\gamma = 4, h_1 = 4, g = -4, \gamma' = 0$: this case is very close to the first-order wetting transition) and for a case deep in the wet phase ($\gamma = 4$, $h_1 = 8$, $g = -4$, $\gamma' = 0$). While the results in Figures 5b, 9 employ the cell dynamics method with a rather coarse discretization, the fine mesh size employed for Figure 11 clearly reveals that the shape of $\phi_{av}(Z,\tau)$ is not at all the simple sinusoidal form yielded by the linearized theory, equation (70): rather Figure 11a suggests a nonlinear shape near the surface describable by a form $\phi_{av}(Z,\tau) \approx -\tanh(Z - Z_0(\tau))$, with an inflection point $Z_0(\tau)$ that slowly moves away from the surface but presumably saturates at a finite equilibrium distance Z_0^{eq} as $\tau \to \infty$. In contrast, for the case in the wet region of the surface (Fig. 11b) one recognizes the characteristic two-step profile: $\phi_{av}(Z,\tau)$ at $Z = 0$ starts at a value larger than unity (i.e., the order parameter at the surface is enhanced beyond its value at the coexistence curve in the bulk), decays on a scale of unity (i.e., about the bulk correlation length, remembering the rescaling of equation (20)) to unity, and then again a profile $\phi_{av}(Z,\tau) \approx -\tanh(Z - Z_0(\tau))$ starts,

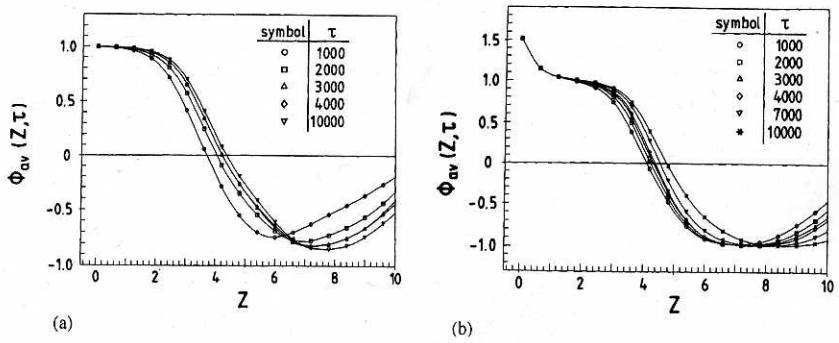

Fig. 11: Averaged order parameter profiles $\phi_{av}(Z,\tau)$ plotted vs. Z for several different scaled times τ after the quench, showing only the region close to the wall, and taking the parameters $\gamma = 4, \gamma' = 0, g = -4, h_1 = 4$ (a) or $h_1 = 8$ (b), respectively. In the numerical implementation of the continuum model represented by Eqs. (19), (41) and (42) a fine mesh is used $\{\Delta\tau = 0.001, \Delta X = 0.4\}$, unlike Fig. 9 which refers to the same parameters as case (a) but uses a coarser mesh $(\Delta X = 1.5, \Delta\tau = 0.05)$. From Puri and Binder [82].

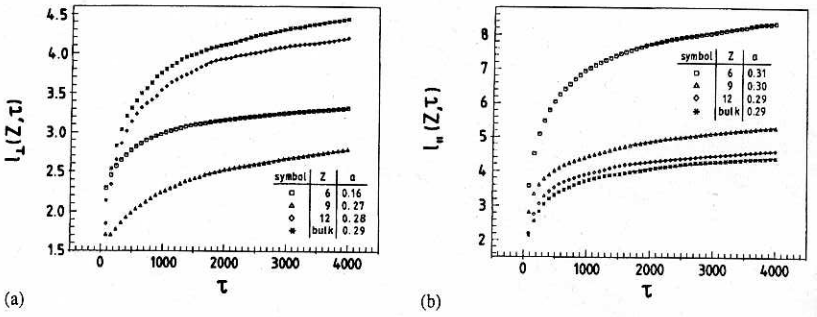

Fig. 12: Perpendicular length scale $l_\perp(Z,\tau)$ (a) and parallel length scale $l_\parallel(Z,\tau)$ (b) plotted vs. scaled time, for the choice of parameters $\gamma = 4$, $\gamma' = 0$, $g = 4$ and $h_1 = 4$. Three choices of Z are shown in each case, and the time evolution of a corresponding bulk system is shown for comparison. The table quotes the effective exponent a of a fit to a power law, $l(Z,\tau) \propto \tau^a$, including times for $\tau > 1600$ only. From Puri and Binder [82].

but how it is more plausible that $Z_0(\tau\to\infty) \to \infty$ (though the growth of the thickness of this wetting layer is presumably only logarithmic in time, $Z_0(\tau) \propto \ln\tau$ as $\tau \to \infty$, consistent with the growth of wetting layers at the coexistence curve [139–143]).

This slow dynamics of the wetting layer also leads [82] to a reduction of the length scale $l_\perp(Z,\tau)$, equation (76) in comparison with the length scale in the bulk, Figure 12a. In contrast, the length scale $l_\parallel(Z,\tau)$ is enhanced in comparison with $l_b(\tau)$. In view of equations (2)–(5) an analysis of these data in terms of power laws was attempted [82],

$$l_\parallel(Z,\tau) \propto \tau^a, \quad l_\perp(Z,\tau) \propto \tau^a, \tag{81}$$

where a is an "effective exponent" that may both depend on Z and on the time interval that is fitted. It is seen that within the accuracy of the fit for $l_\parallel(Z,\tau)$ one finds a close to 1/3, irrespective of Z. Note that it is rather typical for spinodal decomposition in the bulk [3, 4, 5, 6, 7, 28, 29, 30, 132] that the asymptotic Lifshitz-Slezov [22, 23] exponent $a = 1/3$ (eq. (2)) is only seen for extremely late times, and smaller effective exponents between 1/4 and 1/3 are seen at not so late times. In contrast, for $l_\perp(Z,\tau)$ and Z in the surface region much smaller effective exponents like $a \approx 0.16$ are seen, which may result from the fact that the slowly growing wetting layer enforces near the wall a layered structure (with a depletion layer following the enrichment layer, etc.) and thus the growth of $l_\perp(Z,\tau)$ is slowed down.

These findings are compatible with some experiments (e.g. Fig. 4b) and with numerous related simulations of slightly different models which we discuss now [71, 75, 76, 80, 81]. Brown and Chakrabarti [71] included the noise term $\eta_T(\vec{x},t)$ (eq. (23)–(25)) in their model, unlike Puri and coworkers [70, 77, 82, 83] who omitted the noise term, which is believed to be appropriate for the late stages of growth for which thermal fluctuations should be irrelevant [7]. The advantage of keeping the thermal noise terms is that the initial stages of phase separation can also be described, but the disadvantage is that it is much harder to obtain data of statistical quality comparable to those shown in Figure 12 in the same range of times. Brown and Chakrabarti [71] consider the case of rather weak surface fields, where no wetting layer develops at the wall, but rather only somewhat elongated domains form paralled to the wall, i.e. $l_\parallel(Z,\tau) > l_\perp(Z,\tau)$ consistent with what has been said above. They find that the length scale $Z_0(\tau)$ where $\phi_{av}(Z,\tau)$ first changes its sign behaves as $Z_0(\tau) \propto \tau^{1/3}$, and suggest a simple scaling $\phi_{av}(Z,\tau) = \phi(Z/Z_0(\tau))$. As is clear from the above discussion, the latter statement is not true for strong surface fields, where $Z_0(\tau)$ grows much slower with time (perhaps even only logarithmic, $Z_0(\tau) \propto \ln\tau$, for short range surface forces). For the case of "surface-induced nucleation" Brown *et al.* [88] find a crossover from a law $Z_0(\tau) \propto \tau^{1/3}$ to $Z_0(\tau) \propto \tau^{1/6}$, however. In this study, a metastable binary mixture in contact with a wall is considered, for a case where nucleation of the preferred phase at the surface is greatly facilitated in comparison with the bulk.

A very complete study of surface effects on spinodal decomposition was attempted by Marko [76], applying the same cell dynamics technique [130] as Puri *et al.* [70, 77, 82, 100], but including a noise term similar to Brown and Chakrabarti [71], and considering the crossover from large noise to small noise. Marko's work [76] contains both simulations and very interesting phenomenological discussions both on short range and on long range surface forces, including even hydrodynamic flow. While most of his numerical results are also compatible with a behavior $l(\tau) \propto \tau^{1/3}$, except in the case of weak noise and strong surface fields where he finds the formation of a flat surface enriched layer, of exactly the same type as presented in Figures 5, 9, 11, which Marko [76] calls "plating" of the surface, where a much slower growth of the thickness of the surface domains is predicted, in agreement with the results of Puri *et al.* [70, 77, 82] presented in more detail above. It should be noted, however, that typically an average over a few runs was only performed [76], unlike the large sample of at least 50 runs used by Puri *et al.* [82], and hence the statistical accuracy of the data on $l(\tau)$ is somewhat uncertain.

Apart from these studies of the coarse-grained continuum model, equation (19), there have also been numerical studies of more microscopic models [80, 81]. Sagui *et al.* [80] presented a very interesting Monte Carlo study of an Ising lattice model such as shown in Figure 7 (or eqs. (43)–(48), respectively), choosing the Kawasaki [131] spin exchange algorithm similar to Monte Carlo studies of spinodal decomposition in the bulk [132]. They extract a length scale $l_\parallel(Z,\tau)$ from a Fourier transform of the correlation function $G_\parallel$ (eq. (74)) and find that for strong surface exchange ($J_s/J = 10$) the growth of the surface domains is significantly faster, $l_\parallel(Z \to 0,\tau) \propto \tau^{1/2}$, while in the bulk still Lifshitz-Slezov type growth $\{l_b(\tau) \propto \tau^{1/3}\}$ is observed.

While the study of Sagui *et al.* [80] possibly could model surface effects for a solid alloy, Ma *et al.* [81] presented molecular dynamics simulations of a binary Lennard-Jones fluid mixture phase separating in the presence of a wall. Their study showed surface-directed spinodal decomposition in qualitative agreement with experiment [66] and the simulations of the coarse grained models [70, 71, 76]. However, such molecular dynamics simulations are still technically too demanding [33] to allow quantitatively significant studies of growth laws yet.

An important aspect of the coarsening behavior in spinodal decomposition is not only the growth law of the characteristic length scales (eqs. (2)–(5), (81)) but also the question whether the structure factor exhibits a simple scaling behavior, as written in equation (1). This scaling behavior is equivalent to a simple scaling of the correlation function, i.e. in the bulk we have [3, 4, 5, 7]

$$G_b(\vec{X},\tau) \equiv \langle \phi(\vec{X},\tau)\phi(0,0)\rangle - \langle \phi(\vec{X},\tau)\rangle\langle \phi(\vec{X},0)\rangle = \tilde{G}_b\{X/l_b(\tau)\}, \tag{82}$$

and similarly we may assume in the presence of a surface [82]

$$G_\parallel(R,Z,\tau) = \tilde{G}_\parallel\{R/l_\parallel(Z,\tau)\}. \tag{83}$$

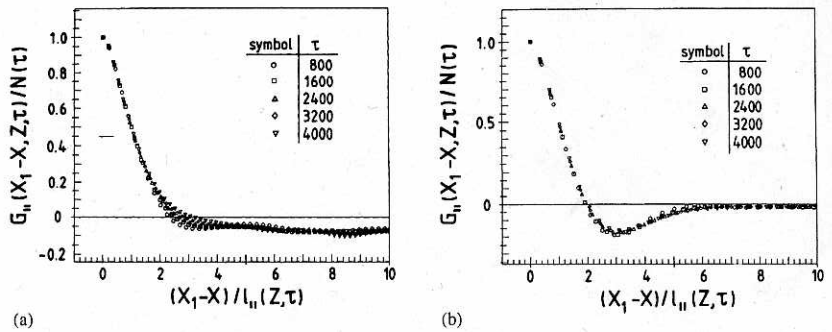

Fig. 13: Normalized correlation functions $G_\parallel(X_1 - X, Z, \tau)/N(\tau)$ where the normalization factor $N(\tau) = G_\parallel(0, Z, \tau)$ plotted vs. the scaling variable $(X_1 - X)/l_\parallel(Z,\tau)$ for $Z = 6$ (a) and $Z = 42$ (b), for the same choice of parameters as in Fig. 12. Five scaled times τ are included and distinguished by different symbols. From Puri and Binder [82].

A test of equation (83) shows [82] (Fig. 13) that such a scaling in the surface region works only approximately and the shape of the scaling function $\tilde{G}_{\parallel}$ seems to differ appreciably from $\tilde{G}_b$.

All the results described so far refer to short range surface forces which are fairly natural in the context of alloy models such as shown in Figure 7, but less natural for fluids in contact with walls where rather long range van der Waals forces are expected to occur [53, 54, 55, 56, 57, 144]. Such forces have been included both in treatments of the phenomenological Ginzburg-Landau equation (eq. (19)) [71, 76, 100] and in Monte Carlo studies of microscopic models [145]. While in the case where these long range forces are relatively weak, the behavior is not much different from the short range case [71, 76], the slow growth of the thickness of the wetting layer that was found for strong surface forces [70, 82] is considerably speeded up in the long range case [100]. Choosing a surface potential $V_s(Z) \propto Z^{-n}$ with $n = 1, 2, 3$, one finds [100] a growth of the length scale $R_1(\tau) \propto \tau^{x(n)}$ with a growth exponent $x(n)$ that depends on n, Figure 14. While for the growth of wetting layers in thermal equilibrium a qualitatively similar behavior occurs [140, 141, 142] $\{x(n) = 1/4,\ 1/6$ and $1/8$ for $n = 1, 2, 3$ if the order parameter is conserved [141] while $x(n) = 1/2, 1/3$ and $1/4$ if it is not conserved [140]$\}$, the results for $x(n)$ shown in Figure 14 still lack any theoretical explanation. Another puzzling feature is the apparent crossover of the growth of the length scale $l_{\parallel}(Z, \tau)$ from a law close to $l_{\parallel}(Z, \tau) \propto \tau^{1/3}$ to $l_{\parallel}(Z, \tau) \propto \tau^{1/2}$ (Fig. 15). At the same time, $L_{\perp}(Z, \tau)$ seems to get pinned! An analytic understanding of these results would be very desirable.

As a final topic of this section we briefly discuss work where phase separation in thin films with two equivalent walls is simulated [83, 117]. It turns out that the behavior of the local correlation functions $G_{\parallel}(R, Z, \tau)$ is very similar to that of the semi-infinite case.

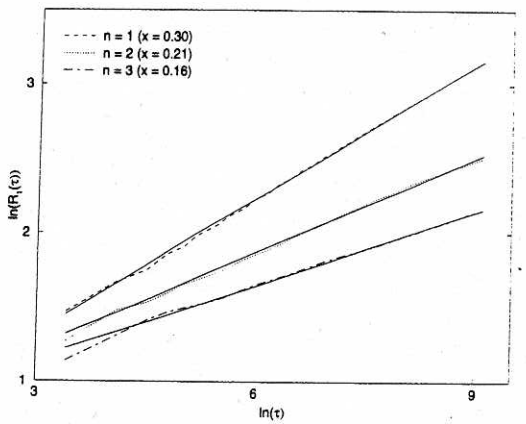

Fig. 14: Log-log plot of the first zero $R_1(\tau)$ of the profile $\phi_{av}(Z, \tau)$ versus τ, for surface potentials $V(Z) = h_1 Z^{-h}$ with $n = 1, 2, 3$, $h_1 = 8$, $g = -4$, $\gamma = 4$, $\gamma' = 0$. The straight lines show fits $R_1(\tau) \propto \tau^{x(n)}$, the exponents $x(n)$ are quoted in the figure. From Puri *et al.* [100].

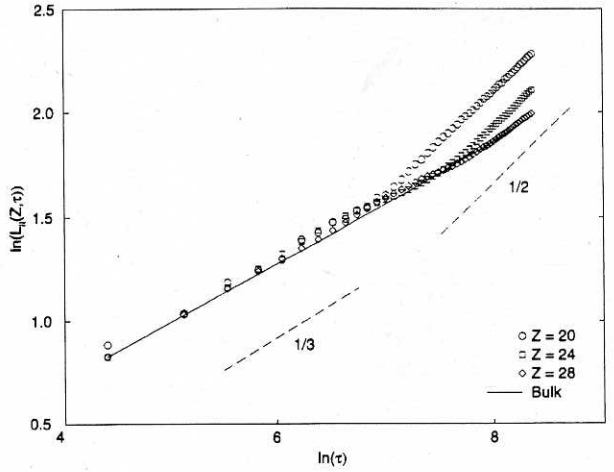

(a)

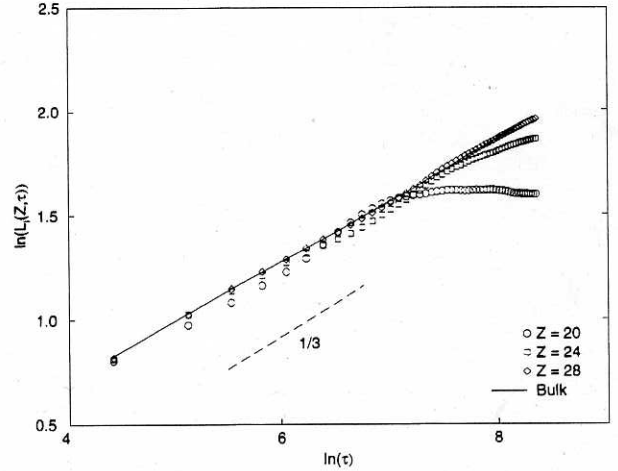

(b)

Fig. 15: Log-log plot of $L_{\parallel}(Z, \tau)$vs. τ (a) and $L_{\perp}(Z, \tau)$ vs τ (b), for the case $n = 3$ and other parameters as shown in Fig. 14. Straight lines with slope 1/3 (and slope 1/2 in case (a)) are shown for comparison. Three values of Z are distinguished by different symbols. From Puri *et al.* [100].

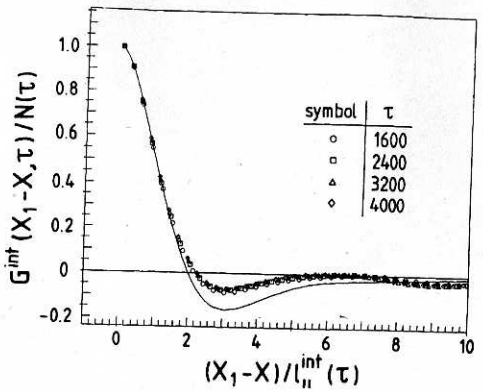

Fig. 16: Integrated correlations $G^{int}(X_1 - X, \tau)$ [eq. (84)], normalized by their maximum values $N(\tau) = G^{int}(0,\tau)$ plotted vs. $(X_1 - X)/l^{int}(\tau)$ for four different times τ. All data are for film thickness $D = 30$, and parameters $h_1 = 4, \gamma = 4, g = -4, \gamma' = 0$. Full curve shows $\tilde{G}_b$. From Puri and Binder [83].

However, for a thin film of thickness D it also makes sense to consider quantities that are integrated over the whole film, corresponding to experiments where one has a lateral resolution only and averages in vertical direction. One defines such an integrated correlation as [83]

$$G^{int}(R, \tau) = \frac{1}{D}\int_0^D G_{\parallel}(R, Z, \tau) dZ \tag{84}$$

and again an integrated length scale can be defined in analogy with equation (75)

$$G^{int}(l^{int}(\tau), \tau) = G^{int}(0, \tau)/2. \tag{85}$$

Figure 16 shows that a scaling relation analogous to equation (83) seems to work rather well for $G^{int}(R, \tau)$, but the scaling function differs appreciably from $\tilde{G}_b$, although for $D \to \infty$ it approaches the latter. Another interesting consequence of the "wetting" layers at the walls of the thin film is that the scaling function $\tilde{S}$ (eq. (1); this is defined here for a wavevector $\tilde{q}$ oriented parallel to the walls) differs appreciably from the bulk as well, for small D the minimum for $q \to 0$ seems to be suppressed altogether [83].

5. Spinodal decomposition in cylindrical pores

We consider first the equilibrium structure of a binary mixture in a cylindrical tube of diameter D and length $L_{\parallel} > > D$ and assume that D is large enough so that $\xi_{\parallel}$ (eq. (7)) is so large that $\xi_{\parallel} > > L_{\parallel}$, so that the absence of true phase transitions in one-dimensional geometry can be ignored. If we are at temperatures where the wall of the pore wets the B-rich phase of the mixture, we expect in equilibrium a tube-like configuration [113]: the walls of the pore are coated with a B-rich layer, and the interior of the pore contains a (cylindrical) domain of the A-rich phase. Note that this state of the system develops

smoothly (without any sharp phase transition) from the one phase region, as the temperature is lowered. Qualitatively, a cross section of the system looks as Figure 2c. However, as metastable states we may encounter "capsules" of length $l < < L_{\parallel}$ which slowly coarsen as time passes. Similarly, at conditions where the walls of the pore are nonwet, thermal equilibrium would require (for $T < T_{cb}$) phase coexistence of two domains inside the pore, say, an A-rich phase on the left separated from a B-rich phase on the right by a single A–B interface. Again one may expect a metastable state with many much smaller cylindrical domains (called "plugs") which all have diameter D now, and also should slowly coarsen [113]. However, for certain conditions a stable equilibrium can exist with a single elongated capsule in the system, whose radius then differs from the radius of the tube (which simply is fixed in terms of the average composition and the lever rule, if one can equate the compositions of the two coexisting phases to their bulk values). Thus, in the equilibrium phase diagram one predicts transitions from "plug" to "capsule", "plug" to "tube", and "capsule" to "plug", respectively. The details of this behavior clearly are sensitive to the balance between the surface forces from the walls of the pore and the interfacial tension. Since in a finite pore there is also some surface enrichment or depletion in the plug state, in the opinion of this author the transition from "plug" to "capsule" should be rounded (and for $L_{\parallel} \to \infty$ the transition from "tube" to "plug" or "capsule" also is rounded, due to the existence of a finite correlation length $\xi_{\parallel}$). However, based on Monte Carlo studies of Ising models Liu and Grest [114] claim that all these transitions are sharp: the "capsule" to "tube" transition is interpreted as an interfacial shape transition, the other transitions are associated with the wetting transition of the semi-finite system. In view of the rather large errors with which these transition are located from the Monte Carlo work [114] supplementary analytic evidence would clearly be very desirable to clarify the question of the sharpness of these transitions.

Dynamics of phase separation in this pore geometry has been treated by Monte Carlo methods [115], simulation of the nonlinear Ginzburg Landau model including the thermal noise term [117], and molecular dynamics simulations [118, 119]. These studies gave evidence that metastable "plug" configurations are indeed formed, and sometimes evidence of tubes also is reported. While the molecular dynamics method in principle is superior, as it automatically includes all hydrodynamics effects, in practice the results [118, 119] are only rather qualitative, since only rather small systems could be studied, and at best an ensemble average over very few runs can be performed. Thus all the reports on the values of the growth exponent for the various conditions have to be taken with great precaution [146].

Of course, the cylindrical pore is mostly considered as a generic model for the pore structure that occurs in real porous media such as Vycor glass. Such pores in real media are contorted and fluctuate in their diameter and have junctions etc. For two-dimensional pores (with one-dimensional walls), Zhang and Chakrabarti [119] have considered a few special geometries of this kind. In addition, simulations have been carried out also for two-dimensional caricatures of the random Vycor-like geometry [147]. It was found that the kinetics of domain growth dramatically slows down as the average size of the domains becomes comparable to the average radius of the pores [147].

6. Concluding remarks

In this review, we have emphasized that spinodal decomposition in confined geometry involves a delicate interplay between the wetting phenomena often induced by the confining walls and the coarsening that would occur in the decomposing mixture also in the bulk. Surface-directed spinodal waves, which are observed in the early stages of the process [64, 66, 74] and are accessible to the theoretical modeling [70, 71, 76, 84, 96], have created much interest in the subject and hence have been emphasized here, but really are only one facet out of many related puzzling phenomena. In the present section, we draw attention to some problems which have been out of the main focus of this article but which clearly are of great interest.

One important phenomenon is that in thin fluid films enclosed between plates there are hydrodynamic mechanisms of spinodal decomposition leading to a much faster growth than in the bulk [68, 69, 91, 148, 149]. Wiltzius *et al.* [68, 69, 79] suggested an universal growth law $l(t) \propto t^{3/2}$ for a surface domain growth which has found much theoretical attention [76, 78, 81, 98] (notwithstanding the fact that there are also experimental observations which find either [150] the conventional power law $l(t) \propto t$, or [151] no power law behavior at all!) Troian [78] proposed a model in which the fast mode results from the geometrical constraint of three-dimensional growth near a two-dimensional surface coated by a wetting layer, increasing the exponent due to coalescence of anisotropic domains. However, assumptions made in this treatment have been exposed to various criticisms [76, 81, 98]. An interesting alternative explanation due to Tanaka [98] proposes that this growth law $l(t) \propto t^{3/2}$, which is faster than any growth law discussed for the bulk (eqs. (2)–(5)) is due to the hydrodynamic spreading of a more wettable fluid phase on a two-dimensional solid surface via bicontinuous fluid tubes [92]. Tanaka [98] also presents arguments that at very late times there should be a crossover to a law $l(t) \propto t$ again, as observed by Harrison *et al.* [149]. Thus, it could be that this last regime corresponds to the observations of Guenoun *et al.* [150]. However, studying phase separation in strictly two-dimensional fluid mixtures (this is possible by considering binary mixtures of amphiphiles at the air-water interface that undergo phase separation [152, 153]) evidence for a growth law $l(t) \propto t^n$ with $n = 0.28$ was presented, for a situation where the volume fraction of the minority phase was $\phi \approx 0.25$. In the opinion of the present author, still more work is needed to clarify the role of hydrodynamic mechanisms under confinement, considering the effects of boundary conditions at the confining surfaces, volume fraction of the minority phase, ratio of viscosities of the two phases, etc. Even for strictly two-dimensional systems the effects on hydrodynamics on the growth laws are controversial [26, 27, 33, 156, 157, 158], as discussed above.

Also in one-dimensional capillaries the hydrodynamic mechanisms have very interesting effects. Tanaka [73, 87, 116] pointed out that the "tube" configuration that initially forms becomes unstable and eventually a stable bamboolike structure is formed, implying that this final structure is determined kinetically, but not thermodynamically.

Even if the simple concepts emphasized in the present article are appropriate, namely formation of surface-directed spinodal waves which later coarsen, in a thin film geometry one has to worry about the interference of the patterns originating from both

surfaces. While in the simulation presented in Figure 5 for the time range presented this was not a problem, experimentally conditions can be reached when this matters [64, 75, 89]. And special effects may be created by a particular preparation of the initial state: If one starts with a multilayer structure, it may happen that every second layer gets dissolved and the structure coarsens by "period doubling" [86] rather than by an uniform power-law type growth law; when one starts with an initially unstable bilayer [154], one finds a decay via an inhomogeneous phase of growing droplets but the final stay may be an inverted bilayer ("surface phase inversion" [154]).

We also emphasize that a systematic variation of both film thickness D and volume fraction ϕ for the same model system would be highly desirable. This systematic variation, to our knowledge, has neither been done in the numerical modeling nor in experiments: Krausch *et al.* [85] have presented a very comprehensive variation of ϕ but did not vary the film thickness; Sung *et al.* [97] changed the film thickness but did not investigate the change of phase diagram with thickness systematically and did not vary the volume fraction. Krausch *et al.* [85] found that the surface spinodal waves are shallower for the case of off-critical compositions than for critical ones, and they pointed out a characteristic surface-induced asymmetry of growth: the wetting layer grows slower if the minority phase wets the surface than in the reverse situation.

Particularly interesting are the claims of Sung *et al.* [96] who suggest that they see the crossover from three-dimensional coarsening to two-dimensional coarsening (with a growth exponent of 0.44 ± 0.02 which needs explanation, however) as they reduce the film thickness from $D = 1000$ Å to $D = 200$ Å (for a polystyrene-polybutadiene polymer blend). An unexplained feature of their results, however, is that their power laws are at best observed a decade in domain size and then pinning of the size suppresses further growth. Note also that unlike numerical work discussed here this experiment refers to a case where D is less than the wavelength of surface-induced spinodal decomposition.

In conclusion, then, it can be said that for the purely diffusive Cahn-Hilliard-type model of spinodal decomposition, in the absence of hydrodynamic effects, and assuming short range forces due to the walls, phase separation in confined geometry is rather well understood: for weak surface fields, there is a uniform coarsening of the initially appearing surface-induced spinodal waves according to a growth law $l(\tau) \propto \tau^{1/3}$, parallel and perpendicular lengths scale in the same way. Despite the fact that in real fluid mixtures hydrodynamic effects to some extent always are present and one has presumably long range surface effects, this behavior is also broadly observed in experiments [64, 74, 85] though there it clearly is not the whole story, as emphasized above. For strong surface fields, there is a strong concentration oscillation normal to the surface and the slower growth of wetting layers creates an anisotropy of growth behavior [82, 83, 100] (the perpendicular length scale $l_\perp(\tau)$ exhibits slower growth rather than the parallel length scale $l_\parallel(\tau)$). Also such a situation may have been realized experimentally [94]. But obviously both more theoretical and experimental work is needed to reach a full understanding of the interplay of finite size and surface effects on structure formation during spinodal decomposition. A particular intriguing

generalization–disregarded here completely— is the possibility that lateral phase separation in a thin binary fluid film with an upper free surface induces a roughening of the latter [93, 155], which is of interest to create patterned substrates for technological applications.

Acknowledgements

The author is very grateful to H. L. Frisch, P. Nielaba, and S. Puri for very fruitful collaborations on work which was crucial for the present review. He is indebted to Prof. G. Krausch for numerous stimulating and useful discussions and his permission to reproduce Figure 4.

References

[1] Cahn, J. W., Hilliard, J. E., Free energy of a nonuniform system. I-Interfacial free energy, J. Chem. Phys.; 28 (1958), 258–267.
[2] Cahn, J. W., On spinodal decomposition, Acta Metall., 9 (1961), 795–801.
[3] For reviews, see Gunton, J. D., San Miguel, M., Sahni, P. S., The dynamics of first-order transitions, in: Phase Transitions and Critical Phenomena, Vol. 8, Eds. C. Domb, J. L. Lebowitz, pp. 267–466, Academic Press, London, 1983, and Refs. 4–7.
[4] Komura, S., Furukawa, H. (eds.) Dynamics of Ordering Processes in Condensed Matter, pp. 1–574, Plenum Press, New York, 1988.
[5] Binder, K., Spinodal decomposition, in: Materials Science and Technology, Vol. 5: Phase Transformations in Materials, Eds. R. W. Cahn, P. Haasen, E. J. Kramer, pp. 405–471, VCH, Weinheim, 1991.
[6] Kostorz, G., Phase separation and structural defects studied by scattering techniques, Physica Scr., T 49, (1993), 636–643.
[7] Bray, A. J., Theory of phase ordering kinetics, Adv. Phys., 43 (1994), 357–459.
[8] Zettlemoyer, A. C., Nucleation, pp. 1–365, M. Dekker, New York, 1969.
[9] Abraham, F. F., Homogeneous Nucleation Theory, pp. 1–263, Academic Press, New York, 1974.
[10] Binder, K., Stauffer, D., Statistical theory of nucleation, condensation and coagulation, Adv. Phys., 25 (1976), 343–396.
[11] Wagner, R., Kampmann, R., Homogeneous second phase precipitation, in: Materials Science and Technology, Vol. 5: Phase Transformations in Materials, Eds. R. W. Cahn, P. Haasen, E. J. Kramer, pp. 213–303, VCH, Weinheim, 1991.
[12] Binder, K., Time-dependent Ginzburg-Landau theory of non-equilibrium relaxation, Phys. Rev. B, 8 (1973), 3423–3438.
[13] Langer, J. S., Metastable states, Physica, 73 (1974), 61–72.
[14] Binder, K., Collective diffusion, nucleation, and spinodal decomposition in polymer mixtures, J. Chem. Phys., 79 (1983), 6387–6409; Binder, K., Nucleation barriers, spinodals, and the Ginzburg criterion, Phys. Rev. A, 29 (1984), 341–349.
[15] Binder, K., Decay of metastable and unstable states: Mechanisms, concepts, and open problems, Physica A, 140 (1986), 35–43.
[16] Cahn, J. W., Hilliard, J. E., Free energy of a nonuniform system. III. Nucleation in a two-component incompressible fluid, J. Chem. Phys., 31, (1959), 688–699.
[17] Klein, W., Unger, C., Pseudospinodals, and nucleation, Phys. Rev. B, 28 (1983), 445–448.
[18] Bates, F. S., Wiltzius, P., Spinodal decomposition of a symmetrical critical mixture of deuterated and protonated polymer, J. Chem. Phys., 91 (1989), 3258–3274; Müller, G., Schwahn, D., Eckerlebe, H., Rieger, J., Springer, T., Effect of the Onsager coefficient and internal relaxation modes on spinodal decomposition in the high molecular isotopic blend polystyrene, deutero-polystyrene studied with small angle neutron scattering, J. Chem. Phys., 104 (1996), 5326–5337.

[19] For a recent review, see Hashimoto, T., Structure of polymer blends, in: Materials Science and Technology, Vol. 12: Structure and Properties of Polymers, Eds. R. W. Cahn, P. Haasen, E. J. Kramer, pp. 251–300, VCH, Weinheim, 1993.
[20] Binder, K., Stauffer, D., Theory for the slowing down of the relaxation and spinodal decomposition of binary mixtures, Phys. Rev. Lett., 33 (1974), 1006–1010.
[21] Binder, K., Stauffer, D., Behavior of the electrical resistivity at phase transitions in binary alloys, Z. Phys. B., 24 (1976), 407–415; Binder, K., Billotet, C., Mirold, P., On the theory of spinodal decomposition in solid and liquid binary mixtures, Z. Phys. B, 30 (1978), 183–195.
[22] Lifshitz, I. M., Slezov, V. V., The kinetics of precipitation from supersaturated solid solutions, J. Phys. Chem. Solids, 19 (1961), 35–50.
[23] For a review, see Slezov, V. V., Theory of Diffusive Decomposition of Solid Solutions (Physics Review, Vol. 17, Part 3), pp. 1–213, Harwood Acad. Publ., Basel, 1995.
[24] Binder, K., Theory for the dynamics of "clusters". II Critical diffusion in binary systems and the kinetics of phase separation, Phys. Rev. B, 15 (1977), 4425–4447. Note, however, that logarithmic corrections appear: Rogers, T. M., Desai, R. C., Numerical study of late-stage coarsening for off-critical quenches in the Cahn-Hilliard equation, Phys. Rev. B, 39 (1989), 11956–11964; Yao, J. H., Elder, K. R., Guo, H., Grant, M., Theory and simulation of Ostwald ripening, Phys. Rev. B, 47 (1993), 14110–14125.
[25] Siggia, E., Late stages of spinodal decomposition in binary mixtures, Phys. Rev. A, 20 (1979), 595–605.
[26] San Miguel, M, Grant, M., Gunton, J. D., Phase separation in two-dimensional binary fluids, Phys. Rev. A, 31 (1985), 1001–1005.
[27] Furukawa, H., Effects of inertia on droplet growth in a fluid, Phys. Rev. A, 31 (1985), 1103–1108; Furukawa, H., Role of inertia in the late stage of the phase separation of a fluid, Physica A, 204 (1984), 237–245.
[28] Akcasu, A. Z., Klein, R., A nonlinear theory of transients following step temperature changes in polymer blends, Macromolecules, 26 (1993), 1429–1441.
[29] Furukawa, H., A dynamic scaling assumption for phase separation, Adv. Phys., 34 (1984), 703–750.
[30] Amar, J., Sullivan, F., Mountain, R., Monte Carlo study of growth in the two-dimensional spin exchange kinetic Ising model, Phys. Rev. B, 37 (1988), 196–208; Rogers, T. M., Elder, K. R., Desai, R. C., Numerical study of the late stages of spinodal decomposition, Phys. Rev. B, 37 (1988), 9638–9649; Toral, R., Chakrabarti, A., Gunton, J. D., Late stages of spinodal decomposition in a three-dimensional model system, Phys. Rev. B, 39 (1989), 4386–4394; Roland, C., Grant, M., Monte Carlo renormalization group study of spinodal decomposition: Scaling and growth, Phys. Rev. B, 39 (1989), 11971–11981.
[31] Koga, T., Kawasaki, K., Spinodal decomposition in binary fluids: Effects of hydrodynamic interactions, Phys. Rev. A, 44 (1991), R817–R820; Puri, S., Dünweg, B., Temporally linear domain growth in the segregation of binary fluids, Phys. Rev. A, 45 (1992), R6977–R6980; Valls, O. T., Farrell, J. E., Spinodal decomposition in a three-dimensional fluid model, Phys. Rev. E, 47 (1993), R36–R39; Koga, T., Kawasaki, K., Late stage dynamics of spinodal decomposition in binary fluid mixtures, Physica A, 196 (1993), 389–415; Shinozaki, A., Oono, Y., Spinodal decomposition in 3-space, Phys. Rev. E, 48 (1993), 2622–2654; Bastea, S., Lebowitz, J. L., Domain growth in computer simulations of segregating two-dimensional binary fluids, Phys. Rev. E, 52 (1995), 3821–3826; Alexander, F. J., Chen, S., Grunau, D. W., Hydrodynamic spinodal decomposition: Growth kinetics and scaling functions, Phys. Rev. B, 48 (1993), 634–637.
[32] Sprik, M., Introduction to molecular dynamics methods, in: Monte Carlo and Molecular Dynamics of Condensed Matter, Eds. K. Binder, G. Ciccotti, pp. 43–88, Società Italiana di Fisica, Bologna, 1996.
[33] Furukawa, H., Dynamics of phase separation of a simple fluid mixture: comparison between molecular dynamics and numerical integration of the phenomenological equation, Phys. Rev. E, 55 (1997), 1150–1161.

[34] Nikolayev, V. S., Beysens, D., Guenon, P., New hydrodynamic mechanism for drop coarsening, Phys. Rev. Lett., 76 (1996), 3144–3147.
[35] Mainville, J., Yang, Y. S., Elder, K. R., Sutton, M., Ludwig, K. F., Jr., Stephenson, G. B., X-ray scattering study of early stage spinodal decomposition in $Al_{0.62}Z_{n_{0.38}}$, Phys. Rev. Lett., 78 (1997), 2787–2790.
[36] Onuki, A., Modulated patterns and pinning effect in phase-separating alloys, in: Mathematics of Microstructure Evolution, Eds. L. Q. Chen, B. Fultz, J. W. Cahn, J. R. Manning, J. E. Morral, J. A. Simmons, pp. 87–100, The Minerals, Metals and Materials Society, Washington, 1996.
[37] Paris, O., Fährmann, M, Fratzl, P., Breaking of rotational symmetry during decomposition of elastically anisotropic alloys, Phys. Rev. Lett., 75 (1995), 3458–3461; Fährmann, M., Fratzl, P., Paris, O., Fährmann, E., Johnson, W. C., Influence of coherency stress on microstructural evolution in model *Ni–Al–Mo* alloys, Acta Metall. Mater., 43 (1995), 1007–1022.
[38] Paris, O., Fährmann, M., Fährmann, E., Pollock, T. M., Fratzl, P., Early stages of precipitate rafting in a single crystal *Ni–Al–Mo* model alloy investigated by small-angle x-ray scattering and TEM, Acta Mater., 45 (1997), 1085–1097.
[39] Tanigushi, T., Onuki, A., Network domain structure in viscoelastic phase separation, Phys. Rev. Lett., 77 (1996), 4910–4913; Tanaka, H., Unusual phase separation in a polymer solution caused by asymmetric molecular dynamics, Phys. Rev. Lett., 71 (1993), 3158–3161; Tanaka, H., Critical dynamics and phase separation kinetics in dynamically asymmetric binary fluids: New dynamic universality class for polymer mixtures or dynamic crossover? J. Chem. Phys., 100 (1994), 5323–5337; Tanaka, H., Araki, T., Phase inversion during viscoelastic phase separation: Roles of bulk and shear relaxation moduli, Phys. Rev. Lett., 78 (1997), 4966–4969.
[40] Tanaka, H., Universality of viscoelastic phase separation in dynamically asymmetric fluid mixtures, Phys. Rev. Lett., 76 (1996), 787–790; Sappelt, D., Jäckle, J., Computer simulation study of phase separation in a binary mixture with a glass-forming component, Physica A, 240 (1997), 453–479; Hikmet, R. M., Callister, S., Keller, A., Thermoreversible gelation of atactic polystyrene: phase transformation and morphology, Polymer, 29 (1988), 1378–1388; Berghmans, S., Mewis, J., Berghmans, H., Meijer, H., Phase behavior and structure formation in solutions of poly (2, 6-dimethyl-1, 4-phenylene ether), Polymer, 36 (1995), 3085–3091.
[41] Jinnai, H., Koga, T., Nishikawa, Y., Hashimoto, T., Hyde, S. T., Curvature determination of a spinodal interface in a condensed matter system, Phys. Rev. Lett., 78 (1997), 2248–2251; Ribbe, A. E., Hashimoto, T., Jinnai, H., Complex image generation in the laser scanning confocal microscope of a polymer blend system, J. Mater. Sci., 31 (1996), 5837–5847; Jinnai, H., Hashimoto, T., Lee, D., Chen, S.-H., Morphological characterization of bicontinuous phase-separated polymer blends and one-phase microemulsions, Macromolecules, 30 (1997), 130–136; White, W. R., Wiltzius, P., Real space measurement of structure in phase separating binary fluid mixtures, Phys. Rev. Lett., 75 (1995), 3012–3015.
[42] Hamano, K., Ushiki, H., Tsunomori, F., Sengers, J. V., Shear effects in a micellar solution near the critical point, Int. J. Thermophysics, 18 (1997), 379–386; Onuki, A., Yamamoto, R., Taniguchi, T., Phase separation in polymer solutions induced by shear, J. Phys. II (France), 7 (1997), 295–304.
[43] For a recent review, see Onuki, A., Phase transitions of fluids in shear flow, J. Phys.: Condens. Matter, 9 (1997), 6119–6157.
[44] Fisher, M. E., Nakanishi, H., Scaling theory for the criticality of fluids between plates, J. Chem. Phys., 75 (1991), 5858–5863; Nakanishi, H., Fisher, M. E., Critical point shifts in films, J. Chem. Phys., 78 (1983), 3279–3293.
[45] Binder, K., Phase transitions in reduced geometry, Ann. Rev. Phys. Chem., 43 (1992), 3–59; Binder, K., Monte Carlo study of thin magnetic Ising films, Thin Solid Films, 20 (1974), 367–381.
[46] Parry, A. O., Evans, R., Influence of wetting on phase equilibria: A novel mechanism for critical-point shifts in films, Phys. Rev. Lett., 64 (1990), 439–442; Parry, A. O., Evans, R.: Novel phase behavior of a confined fluid or Ising magnet, Physica A, 181 (1992), 250–296.
[47] Binder, K., Landau, D. P., Ferrenberg, A. M., Character of the phase transition in thin Ising films with competing walls, Phys. Rev. Lett., 74 (1995), 298–301; Binder, K., Landau, D. P., Ferrenberg, A. M., Thin Ising films with competing walls: A Monte Carlo study, Phys. Rev. E, 51 (1995), 2823–2838; Binder, K., Evans, R., Landau, D. P., Ferrenberg, A. M., The interface localization transition in Ising films with competing walls: Ginzburg criterion and crossover scaling, Phys. Rev. E, 53 (1996), 5023–5034.
[48] Tang, H., Szleifer, I., Kumar, S. K., Critical temperature shifts in thin polymer blend films, J. Chem. Phys., 100 (1994), 5367–5371; Rouault, Y., Baschnagel, J., Binder, K., Phase separation of symmetrical mixtures in thin film geometry, J. Stat. Phys., 80 (1995), 1009–1031; Flebbe, T., Dünweg, B., Binder, K., Phase separation versus wetting: a mean field theory for symmetrical polymer mixtures confined between selectively attractive walls, J. Phys. II (France), 6 (1996), 667–695.
[49] Binder, K., Nielaba, P., Pereyra, V., Phase coexistence in binary mixtures in thin films with symmetric walls: Model calculations for two- and three-dimensional Ising latticcs, Z. Phys. B, 104 (1997), 81–98.
[50] For a review with emphasis on polymeric fluids, see Binder, K.: Phase transitions of polymer blends and block copolymer melts in thin films, Adv. Polm. Sci., in press, 1998.
[51] Binder, K., Critical behavior at surfaces, in: Phase Transitions and Critical Phenomena, Vol. 8, Eds. C. Domb, J. L. Lebowitz, pp. 1–144, Academic Press, London, 1983.
[52] Fisher, M. E., Walks, walls, wetting, and melting, J. Stat. Phys., 34 (1984), 667–729; Fisher, M. E., Interface wandering in adsorbed and bulk phases, pure and impure, J. Chem. Soc., Faraday Trans. 2, 82 (1986), 1569–1603.
[53] de Gennes, P. G., Wetting: statics and dynamics, Rev. Mod. Phys., 57 (1985), 827–863.
[54] Sullivan, D. E., Telo da Gama, M. M., Wetting transitions and multilayer adsorption at fluid interfaces, in: Fluid Interfacial Phenomena, Ed. C. A. Croxton, pp. 45–134, Wiley, New York, 1986.
[55] Dietrich, S., Wetting phenomena, in: Phase Transitions and Critical Phenomena, Vol. 12 Eds. C. Domb, J. L. Lebowitz, pp. 1–218, Academic Press, London, 1988.
[56] Schick, M., Introduction in wetting phenomena, in: Liquids at Interfaces, Eds. J. Charvolin, J.-F. Joanny, J. Zinn-Justin, pp. 415–497, North-Holland, Amsterdam, 1990.
[57] Henderson, D. (Ed.) Fundamentals of Inhomogeneous Fluids, pp. 1–431, M. Dekker, New York, 1992.
[58] Fisher, M. E., The theory of critical point singularities, in: Critical Phenomena, Proc. 1970 E. Fermi Int. School Phys., Ed. M. S. Green, pp. 1–99, Academic Press, London, 1971.
[59] Barber, M. N., Finite size scaling, in: Phase Transitions and Critical Phenomena, Vol. 8, Eds. C. Domb, J. L. Lebowitz, pp. 145–266, Academic Press, London, 1973.
[60] Binder, K., Finite size effects on phase transitions, Ferroelectrics, 73 (1987), 43–67; Binder, K., Finite size effects at phase transitions, in: Computational Methods in Field Theory, Eds. H. Gausterer, C. B. Lang, pp. 59–125, Springer, Berlin, 1992.
[61] Privman, V. (Ed.) Finite Size Scaling and Numerical Simulation of Statistical Systems, World Scientific, Singapore, 1990.
[62] Cahn, J. W., Critical point wetting, J. Chem. Phys., 66 (1977), 3667–3672.
[63] For a recent review, see also Puri, S., Frisch, H. L., Surface-directed spinodal decomposition: Modelling and numerical simulations, J. Phys.: Condens. Matter, 9, 2109–2133, and Ref. 64.
[64] Krausch, G., Surface induced self-assembly in thin polymer films, Mat. Sci. Eng. Rep., 14 (1995), 1–94.
[65] Ball, R. C., Essery, R. L. H., Spinodal decomposition and pattern formation near surfaces J. Phys.: Condens. Matter, 2 (1990), 10303–10320.
[66] Jones, R. A. L., Norton, L. J., Kramer, E. J., Bates, F. S., Wiltzius, P., Surface-directed spinodal decomposition, Phys. Rev. Lett., 66 (1991), 1326–1329.
[67] Binder, K., Frisch, H. L., Dynamics of surface enrichment: A theory based on the Kawasaki spin-exchange model in the presence of a wall, Z. Phys. B., 84 (1991), 403–418.

[68] Wiltzius, P., Cumming, A., Domain growth and wetting in polymer mixtures, Phys. Rev. Lett., 66 (1991), 3000–3003.
[69] Cumming, A., Wiltzius, P., Bates, F. S., Rosedale, J. H., Light-scattering experiments on phase-separation dynamics in binary fluid mixtures, Phys. Rev. A, 45 (1992), 885–897.
[70] Puri, S., Binder, K., Surface-directed spinodal decomposition: Phenomenology and numerical results, Phys. Rev. A, 46 (1992), R4487–R4489.
[71] Brown, G., Chakrabarti, A., Surface-directed spinodal decomposition in a two-dimensional model, Phys. Rev. A, 46 (1992), 4829–4835.
[72] Bruder, F., Brenn, R., Spinodal decomposition in thin films of a polymer blend, Phys. Rev. Lett. 69 (1992), 624–627.
[73] Tanaka, H., Wetting dynamics in a confined symmetric mixture undergoing phase separation, Phys. Rev. Lett. 70 (1993), 2770–2773; Tanaka, H., Interplay between phase separation and wetting for a polymer mixture confined in a two-dimensional capillary: Wetting induced domain ordering and coarsening, Europhys. Lett., 24 (1993), 665–671.
[74] Krausch, G., Dai, C.-A., Kramer, E. J., Bates, F. S., Real space observation of dynamic scaling in a critical polymer mixture, Phys. Rev. Lett., 71 (1993), 3669–3672.
[75] Krausch, G., Dai, C.-A., Kramer, E. J., Marko, J. F., Bates, F. S., Interference of spinodal waves in thin polymer films, Macromolecules, 26 (1993), 5566–5571.
[76] Marko, J. F., Influence of surface interactions on spinodal decomposition, Phys. Rev. E, 48 (1993), 2861–2879.
[77] Puri, S., Frisch, H. L., Dynamics of surface enrichment. Phenomenology and numerical results above the bulk critical temperature, J. Chem. Phys., 99 (1993), 5560–5570.
[78] Troian, S., Coalescence-induced domain growth near a wall during spinodal decomposition, Phys. Rev. Lett., 71 (1993), 1399–1402; Troian, S., Domain growth near a wall in spinodal decomposition: Troian replies, Phys. Rev. Lett., 72 (1994) 3739.
[79] Shi, B. Q., Harrison, C., Cumming, A., Fast-mode kinetics in surface-mediated phase-separating fluids, Phys. Rev. Lett., 70 (1993), 206–209.
[80] Sagui, C., Somozo, A. M., Roland, C., Desai, R. C., Phase separation in the presence of a surface, J. Phys. A: Math. Gen., 26 (1993), L1163–L1168.
[81] Ma, W. J., Keblinski, P., Maritan, A., Koplik, J., Banavar, J. R., Composition waves in confined geometries, Phys. Rev. E, 48 (1993), R2362–R2365; Keblinski, P., Ma, W. J., Maritan, A., Koplik, J., Banavar, J. R., Domain growth near a wall in spinodal decomposition, Phys. Rev. Lett., 72 (1994), 3738; Keblinski, P., Ma, W. J., Maritan, A., Koplik, J., Banavar, J. R., Molecular dynamics of phase separation in narrow channels, Phys. Rev. E, 47 (1993), R2265–R2268.
[82] Puri, S., Binder, K., Surface efforts on spinodal decomposition in binary mixtures and the interplay with wetting phenomena, Phys. Rev. E, 49 (1994), 5359–5377.
[83] Puri, S., Binder, K., Surface-directed spinodal decomposition in a thin film geometry: A computer simulation, J. Stat. Phys., 77 (1994), 145–172.
[84] Vaksman, M. A., Mc Mullen, W. E., Phase separation dynamics of model thin films, Phys. Rev. E (1994), 4724–4727.
[85] Krausch, G., Kramer, E. J., Bates, F. S., Marko, J. F., Brown, G., Chakrabarti, A., Surface-induced asymmetries during spinodal decomposition in off-critical polymer mixtures, Macromolecules, 27 (1994), 6768–6776.
[86] Krausch, G., Mlynek, J., Straub, W., Brenn, R., Marko, J. F., Order-induced period doubling during surface-directed spinodal decomposition, Europhys. Lett., 28 (1994), 323–328.
[87] Tanaka, H., Dynamic interplay between wetting and phase separation in geometrically confined polymer mixtures, in: Ordering in Macromolecular Systems, Eds. A. Teramoto, M. Kobayashi, T. Norisuje, pp. 291–300, Springer, Berlin, 1994.
[88] Brown, G., Chakrabarti, A., Marko, J. F., Surface-induced nucleation, Phys. Rev. E, 50 (1994), 1674–1677.
[89] Kim, E., Krausch, G., Kramer, E. J., Osby, O. J., Surface-directed spinodal decomposition in the blend of polystyrene and tetramethyl-bisphenol-a polycarbonate, Macromolecules, 27 (1994), 5927–5929.

[90] Krausch, G., Kramer, E. J., Rafailovich, M. H., Sokolov, J., Self-assembly of a homopolymer mixture via phase separation, Appl. Phys. Lett., 64 (1994), 2655–2657.
[91] Pan, Q., Composto, R. J., Phase separation studies of confined thin film polymer blends, Mat. Res. Soc. Symp. Proc., 366 (1995), 27–32.
[92] Tanaka, H., Sigehuzi, T., Spinodal decomposition of a symmetric binary fluid mixture in quasi two dimensions: Local orientational ordering of fluid tubes, Phys. Rev. E, 52 (1994), 829–834.
[93] Straub, W., Bruder, F., Brenn, R, Krausch, G., Bielefeldt, A., Kirsch, A., Marti, O., Mlynek, J. L., Marko, J. F., Transient wetting and 2D spinodal decomposition in a binary polymer blend, Europhys. Lett., 29 (1995), 353–358.
[94] Geoghegan, M., Jones, R. A. L., Clough, A. S., Surface directed spinodal decomposition in a partially miscible polymer blend, J. Chem. Phys., 103 (1995), 2719–2724.
[95] Harrison, C., Rippard, W., Cumming, A., Video microscope and elastic light scattering studies of fast-mode kinetics in surface-mediated spinodal decomposition, Phys. Rev. E, 52 (1995), 723–729.
[96] Frisch, H. L., Nielaba, P., Binder, K., Surface effects on spinodal decomposition in the framework of a linearized theory, Phys. Rev. E, 52 (1995), 2848–2859.
[97] Sung, L., Karim, A., Douglas, J. F., Han, C. C., Dimensional crossover in the phase separation kinetics of thin polymer blend films, Phys. Rev. Lett., 76 (1996), 4368–4371.
[98] Tanaka, H., Simple hydrodynamic model of fast-mode kinetics in surface-mediated fluid phase separation, Phys. Rev. E, 54 (1996), 1709–1714.
[99] Dalnoki-Veress, K., Forrest, J. A., Stevens, J. R., Dutcher, J. R., Phase separation morphology of thin films of polystyrene/polyisoprene blends, J. Polym. Sci.: Part B, Polym. Phys., 34 (1996), 3017–3024.
[100] Puri, S., Binder K., Frisch, H. L., Surface effects on spinodal decomposition in binary mixtures: the case with long-ranged surface fields, Phys. Rev. E, 56 (1997), 6991–7000.
[101] Fischer, H. P., Maass, P., Dieterich, W., Novel surface modes in spinodal decomposition, Phys. Rev. Lett., 79 (1997), 893–896.
[102] Tersoff, J., Surface-confined alloy formation in inmiscible systems, Phys. Rev. Lett., 74 (1995), 434–437.
[103] Blakely, J. M., Segregation to surfaces: dilute alloys of the transition metals. CRC Crit. Rev. Solid State & Mater. Sci. (USA), 7 (1978), 333–355.
[104] Brochard, F., de Gennes, P. G., Phase transitions of binary mixtures in random media, J. Phys. (France) Lett., 44 (1983), L785–L791.
[105] de Gennes, P. G., Liquid-liquid demixing inside a rigid network. Qualitative features, J. Phys. Chem., 88 (1984), 6469–6472.
[106] Maher, J. V., Goldburg, W. I., Pohl, D. W., Lanz, M., Critical behavior in gels saturated with binary liquid mixtures, Phys. Rev. Lett., 53 (1984), 60–63; Goh, M. C., Goldburg, W. I., Knobler, C. M., Phase separation of a binary liquid mixture in a porous medium, Phys. Rev. Lett., 58 (1987), 1008–1011; Dierker, S. B., Wiltzius, P., Random-field transition of a binary liquid in a porous medium, Phys. Rev. Lett., 58 (1987), 1865–1868.
[107] Andelman, D., Joanny, J. F., Metastability and Landau theory for random fields and demixing in porous media, in: Scaling Phenomena in Disordered Systems, Eds. R. Pynn, A. Skjeltorp, pp. 163–170, Plenum Press, New York, 1985.
[108] Goldburg, W. I., Phase separation in porous media, in: Dynamics of Ordering Processes in Condensed Matter, Eds. S. Komura, H. Furukawa, pp. 361–372, Plenum Press, New York, 1988.
[109] Goldburg, W. I., Aliev, F., Wu, X. L., Behavior of liquid crystals and fluids in porous media, Physica A, 213 (1995), 61–70.
[110] Kim, S. B., Ma, J., Chan, M. H. W., Phase diagram of $^3He-{}^4He$ mixture in aerogel, Phys. Rev. Lett., 71 (1993), 2268–2271.
[111] Falicov, A., Berker, A.N., Correlated random-chemical potential model for the phase transitions of helium mixtures in porous media, Phys. Rev. Lett., 74 (1995), 426–429.
[112] Pricaupenko, L., Treiner, J., Phase separation of liquid $^3He-{}^4He$ mixtures: Effect of confinement, Phys. Rev. Lett., 74 (1995), 430–433.

[113] Liu, A. J., Durian, D. J., Herbolzheimer, E., Safran, S. A., Wetting transitions in a cylindrical pore, Phys. Rev. Lett., 65 (1990), 1897–1900.
[114] Liu, A. J., Grest, G. S., Wetting in a confined geometry: A Monte Carlo study, Phys. Rev. A, 44 (1991), R7894–R7897.
[115] Monette, L., Liu, A. J., Grest, G. S., Wetting and domain-growth kinetics in confined geometries, Phys. Rev. A, 46 (1992), 7664–7679.
[116] Tanaka, H., Dynamic interplay between phase separation and wetting in a binary mixture confined in a one-dimensional capillary, Phys. Rev. Lett., 70 (1993), 53–56.
[117] Bhattacharya, A., Rao, M., Chakrabarti, A., Phase separation in binary mixtures confined in a strip geometry, Phys. Rev. E, 49 (1994), 524–530.
[118] Zhang, Z., Chakrabarti, A., Phase separation of binary fluids confined in a cylindrical pore: A molecular dynamics study, Phys. Rev. E, 50 (1994), R4290–R4293.
[119] Zhang, Z., Chakrabarti, A., Phase separation of binary fluids in porous media: Asymmetries in pore geometry and fluid composition, Phys. Rev. E, 52 (1995), 2736–2741.
[120] Uzelac, K., Hasmy, A., Jullien, R., Numerical study of phase transitions in the pores of an aerogel, Phys. Rev. Lett., 74 (1995), 422–425.
[121] Imry, Y. Ma, S.-K., Random-field instability of the ordered state of continuous symmetry, Phys. Rev. Lett., 35 (1975), 1399–1401.
[122] Nattermann, T., Villain, J., Random-field Ising systems: a survey of current theoretical views, Phase Transitions, 11 (1988), 5–51.
[123] Albano, E. V., Binder, K., Heermann, D. W., Paul, W., Kinetics of domain growth in finite Ising strips, Physica A, 183 (1992), 130–147.
[124] Fisher, M. E., Aspects of equilibrium critical phenomena, J. Phys. Soc. Jpn. Suppl., 26 (1969), 87–93; Fisher, M. E., Privman, V., Finite-size effects at first-order transitions, J. Stat. Phys., 33 (1983), 385–417.
[125] Binder, K., Kinetic Ising model study of phase separation in binary alloys, Z. Phys., 267 (1974), 313–322.
[126] Hohenberg, P. C., Halperin, B. I., Theory of dynamic critical phenomena, Rev. Mod. Phys., 49 (1977), 435–479.
[127] Kawasaki, K., Ohta, T., Theory of early stage spinodal decomposition in fluids near the critical point II, Progr. Theor. Phys., 59 (1978), 362–374.
[128] de Groot, S. R., Mazur, P., Non-Equilibrium Thermodynamics, North-Holland, Amsterdam, 1962.
[129] Cook, H. E., Brownian motion in spinodal decomposition, Acta Metall., 18 (1970), 297–306.
[130] Oono, Y., Puri, S., Study of phase-separation dynamics by use of cell dynamical systems, I. Modeling, Phys. Rev. A, 38 (1988), 434–453; Puri, S., Oono, Y., Study of phase-separation dynamics by use of cell dynamical systems. II. Two-dimensional demonstrations, Phys. Rev. A, 38 (1988), 1542–1565.
[131] Kawasaki, K., Kinetics of Ising Models, in: Phase Transitions and Critical Phenomena, Vol. 2, Eds. C. Domb, M. S. Green, pp. 443–501, Academic Press, London, 1972.
[132] Bortz, A. B., Kalos, M. H., Lebowitz, J. L., Zendejas, M. A., Time evolution of a quenched binary alloy: Computer simulation of a two-dimensional model system, Phys. Rev. B, 10 (1974), 535–541; Marro, J., Bortz, A. B., Kalos, M. H., Lebowitz, J. L., Time evolution of quenched binary alloy II. Computer simulation of a three-dimensional model system, Phys. Rev. B, 12 (1975), 2000–2011; Marro, J., Lebowitz, J. L., Kalos, M. H., Computer simulation of the time evolution of a quenched model alloy in the nucleation region, Phys. Rev. Lett., 43 (1979), 282–285; for recent work, see Liverpool, T. P., Correlations in two dimensional domain coarsening, Physica A, 224 (1996), 589–603.
[133] Ginzburg, V. L., Some remarks on second order phase transitions and the microscopic theory of ferroelectrics, Soviet Phys. Solid State, 2 (1960), 1824–1836 [Fiz.tverdogo Tela 2 (1960), 2031–2043].
[134] Carmesin, H.-O., Heermann, D. W., Binder, K., Influence of a continuous quenching procedure on the initial stages of spinodal decomposition, Z. Phys. B, 65 (1986), 89–102.

[135] For this reason we do not discuss further the work of Xiong, G. M., Gong, C. D., Early time spinodal decomposition in the surface layer, Phys. Rev. B, 39 (1989), 9384–9388, who applied a single boundary condition only, violating Eq. (41).
[136] Diehl, H. W., Janssen, H.-K., Boundary conditions for the field theory of dynamic critical behavior in semi-infinite systems with conserved order parameter, Phys. Rev. A, 45 (1992), 7145–7155.
[137] Flynn, C. P., Point Defects and Diffusion, pp. 1–260, Clarendon, Oxford, 1972.
[138] The equations quoted here are a simplified version of the equations solved in Ref. 96, putting $k_{\|} = 0$ and $\kappa' = 0$.
[139] Schmidt, I., Binder, K., Dynamics of wetting transitions: A time-dependent Ginzburg-Landau treatment, Z. Phys. B, 67 (1987), 369–385; Puri, S., Binder, K., Surface effects on kinetics of ordering, Z. Phys. B, 86 (1992), 263–271.
[140] Lipowsky, R., Nonlinear growth of wetting layers, J. Phys. A, 18 (1985), L585–L590.
[141] Lipowsky, R., Huse, D. A., Diffusion-limited growth of wetting layers, Phys. Rev. Lett., 52 (1986), 353–356.
[142] Mon, K. K., Binder, K., Landau, D. P., Monte Carlo simulation of the growth of wetting layers, Phys. Rev. B, 35 (1978), 3683–3685; Mon, K. K., Binder, K., Landau, D. P., Dynamic Monte Carlo simulation of the depinning of domain walls, J. Appl. Phys., 61 (1987), 4409–4410; Binder, K., Growth kinetics of wetting layers at surfaces, in: Kinetics of Ordering and Growth at Surfaces, Ed. M. Lagally, pp. 31–44, Plenum Press, New York, 1990.
[143] Grant, M., Dynamics of roughening and complete wetting, Phys. Rev. B, 37 (1988), 5705–5712.
[144] Israelashvili, J., Intermolecular and Surface Forces, pp. 1–314, Academic Press, London, 1985.
[145] Jiang, Z., Ebner, C., Simulated growth of wetting films with a conserved order parameter, Phys. Rev. B, 39 (1989), 2501–2505.
[146] Ossadnik, P., Gyure, M., Stanley, H. E., Glotzer, S. C., Molecular dynamics simulation of spinodal decomposition in a two-dimensional binary fluid mixture, Phys. Rev. Lett., 72 (1994), 2498.
[147] Chakrabarti, A., Kinetics of domain growth and wetting in a model porous media, Phys. Rev. Lett., 69 (1992), 1548–1551; Lee, J. C., Ordering processes in porous media, Phys. Rev. Lett., 70 (1993), 3599–3602; Grunau, D. W., Lookman, T., Chen, S. Y., Lapedes, A. S., Domain growth, wetting, and scaling in porous media, Phys. Rev. Lett., 71 (1993), 4198–4201.
[148] Bodensohn, J., Goldburg, W. I., Spinodal decomposition between closely spaced plates, Phys. Rev. A, 46 (1992), 5084–5088.
[149] Harrison, C., Rippard, W., Cumming, A., Video microscope and elastic light scattering studies of fast-mode kinetics in surface-mediated spinodal decomposition, Phys. Rev. E, 52 (1995), 723–729.
[150] Guenoun, P., Beysens, D., Robert, M., Dynamics of wetting and phase separation, Phys. Rev. Lett., 65 (1990), 2406–2409; Guenon, P., Beysens, D., Robert, M., Dynamics of interfaces near a wall during phase separation, Physica A, 172 (1991), 137–146.
[151] Katzen, D., Reich, S., Image analysis of phase separation in polymer blends, Europhys. Lett., 21 (1993), 55–60.
[152] Seul, M., Morgan, N. Y., Sire, C., Domain coarsening in a two-dimensional binary mixture: Growth dynamics and spatial correlations, Phys. Rev. Lett., 73 (1994), 2284–2287.
[153] Morgan, N. Y., Seul, M., Structure of disordered droplet domain patterns in a monomolecular film, J. Phys. Chem., 99 (1995), 2088–2095.
[154] Steiner, U., Klein, J., Fetters, L. J., Surface phase inversion in finite-sized binary mixtures, Phys. Rev. Lett., 72 (1994), 1498–1501.
[155] Karim, A., Slawecki, T., Kumar, S. K., Russell, T. P., Satija, S. K., Han, C. C., Liu, Y., Rafailovich, M. H., Sokolov, J., Phase separation induced roughening transition in thin polymer blend films, preprint.